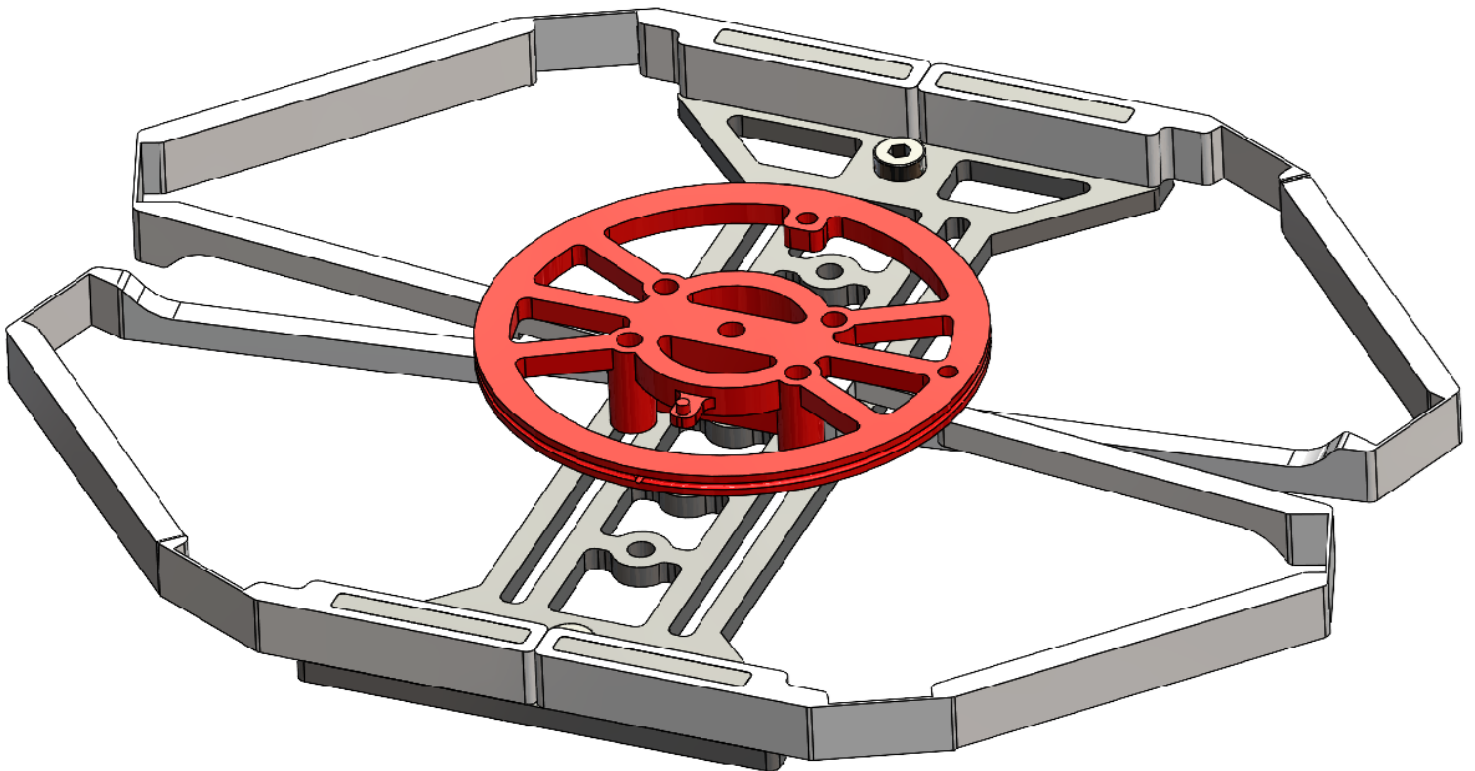


Department of Precision and Microsystems Engineering

Statically Balanced Multi-Degree-of-Freedom Compliant Mechanism utilizing Preload Integration

T. Q. Vis

Report no : 2024.097
Coach : Dr. J. Jovanova
Professor : Prof.dr.ir J.L Herder
Specialisation : MSD
Type of report : Master Thesis
Date : 12-11-2024



Statically Balanced Multi-Degree-of-Freedom Compliant Mechanism utilizing Preload Integration

by

T. Q. Vis

to obtain the degree of Master of Science
at the Delft University of Technology,
to be defended publicly on Tuesday November 12, 2024 at 3:00 PM.

Student number: 4699173
Project duration: September, 2023 – November, 2024
Thesis committee: Prof. dr. ir. J. Herder, TU Delft, chair
Dr. J. Jovana, TU Delft, supervisor
Dr. A. Hunt, TU Delft

An electronic version of this thesis is available at <http://repository.tudelft.nl/>.

Preface

This thesis was written as part of the Master's program in High Tech Engineering within the Department of Precision and Microsystems Engineering (PME) at Delft University of Technology. Initially, it began as a collaboration between the PME and Maritime and Transportation Technology departments, fueled by my interest in compliant mechanisms and soft robotics. What started as an exploration of compliant actuation to enhance soft robotics evolved into a deeper investigation of energy efficiency in compliant mechanisms through static balancing. Although the final project diverged significantly from its original focus, it was rewarding to experience the transformation of this idea and witness the project's evolution. I am deeply grateful not only for the technical knowledge I gained about compliant mechanisms, but also for the personal growth I experienced over this past year.

I would like to express my sincere gratitude to Jovana Jovanova for giving me the opportunity to conduct this research. Her insights during our recurring meetings and encouragement to pursue new ideas were invaluable. I am also deeply grateful to Just Herder, whose guidance and expertise helped shape this project. Our discussions often delved into the technical aspects, emphasizing the value of critical thinking.

A special thanks to my friends for supporting me over these past two years. I deeply appreciate the friendships we've built and your willingness to help with the project whenever possible. I'm also grateful for our time together off campus, giving me valuable breaks from my studies. Finally, I want to thank my parents and sister for their constant support throughout my educational career towards becoming an engineer. I seriously couldn't have achieved this without you!

Tom Vis
Delft, November 2024

Contents

1 MSc Report	1
Introduction	2
Design Methodology	4
Evaluation of Optimized Designs	6
Flexure Arm Design and Prototyping	8
Experimental Validation	10
Experimental Results	11
Discussion	12
Conclusion	14
2 Appendices	17
Appendix A: Reasoning behind the project	18
Appendix B: Working Principle of PRBM	19
Appendix C: Explanation of implemented normalization method and Root-Mean-Square	19
Appendix D: Moment Reduction Plots - Case Study and Compensated Beams	20
Appendix E: Pictures of the Test Setup for Moment Measurements	20
Appendix F: First Iterations of the Mechanism	21
Appendix G: First Prototype of the compensated beams mechanism	22
Appendix H: Material selection of the flexures	22
Appendix I: Difference between unloaded and preloaded flexures	22
Appendix J: Compensated Beams Matlab Script	23
Appendix K: Ansys Code for Force-Displacement on Preloaded Mechanism	26
Appendix L: Ansys Code for Moment-Rotation on Preloaded Mechanism	30
Appendix M: Ansys Code for Unloaded Mechanism	31
3 Literature Review	32
Introduction	34
Search Methodology	35
Compliant Mechanisms for Flexible Robotics	35
Smart Material Actuation for Compliant Mechanisms	39
A Way Forward in Flexible Robotics	42
Conclusion	43

1

MSc Report

To obtain the degree of Master of Science at the Delft University of Technology,
to be defended publicly on:

12 November, 2024, Delft, The Netherlands

Report No: 2024.097

STATICALLY BALANCED MULTI-DEGREE-OF-FREEDOM COMPLIANT MECHANISM UTILIZING PRELOAD INTEGRATION

Tom Q. Vis

Department of Precision and
Microsystems Engineering
Delft University of Technology
Delft, The Netherlands
T.Q.Vis@student.tudelft.nl

Prof.dr.ir. Just L. Herder

Department of Precision and
Microsystems Engineering
Delft University of Technology
Delft, The Netherlands
J.L.Herder@tudelft.nl

Dr. Jovana Jovanova

Department Maritime and
Transportation Technology
Delft University of Technology
Delft, The Netherlands
J.Jovanova@tudelft.nl

ABSTRACT

In mechanical systems, energy efficiency is often reduced by unwanted forces like friction and backlash, which significantly impact performance and, over time, lead to increased wear and maintenance costs. Implementing compliant joints can address these issues, simplifying assembly and improving performance. However, compliant mechanisms introduce higher internal loads due to elastic deformation in the flexures, limiting the range of motion and affecting overall efficiency. One way to solve this is using the principle of static balancing, which ensures that a point of interest remains in equilibrium, meaning that no added forces or moments are needed to keep it at rest at certain positions. This can be done by compensating the internal potential energy, which has been implemented in literature for 1 Degree of Freedom configurations. The goal of this paper was to expand the known method into designing a multi-degree of freedom without the use of external springs. The method was based on applying a preload to the compliant joints in the mechanism and optimize in such a way to create a constant potential energy curve. The model was validated using finite element analysis, prototyping and physical testing. It can be concluded that for the first time, a two degree of freedom statically balanced mechanism has been designed. It has a peak force reduction of 95% and a moment reduction of 80%, while having a range of motion worth 50% of the size of the mechanism. The mechanism can be used in vibration isolators or as fundamental inspiration for new applications where preloading could lead to lower exerted loads and thus improve efficiency.

Keywords: Compliant Mechanism, Statically Balance, Potential Energy, Preloading, Multi-DoF, Flexure, Linkage

1 Introduction

In today's world, efficiency and low power consumption are crucial when developing new technologies. For actuated mechanisms, this means reducing the forces needed to move the structure within its intended range. Methods to accomplish this are zero stiffness or statically balancing applications and while both concepts are related, they differ in their approach to reducing the loads required for movement [1]. Statically balanced systems are designed to counteract the forces due to gravity or other external forces, so the system remains in equilibrium at any position within a given range. This method generally makes use of specific mechanical design, external springs or counterweight to cancel out each other's effects and reduce force input. The goal is to create a constant potential energy curve along the design domain.

Statically balancing is used in literature in multiple types of applications, such as positioning mechanisms [2–4] and gravity balancers [5–11]. These types of mechanisms rely on conventional joints, which come with drawbacks such as friction, backlash, and particle production. In robotics, these issues can lead to decreased accuracy and higher maintenance costs. To address these challenges in high-precision applications, compliant mechanisms are introduced to eliminate these disadvantages. Compliant mechanisms make use of members that are able to bend along their length [12] due to the elastic deformation in the chosen ma-

terial and configuration. This deflection can result in movement with desirable characteristics, such as frictionless motion and little to no assembly necessary. These types of mechanisms have been developed for various applications, including: grasping, locomotion, vibration isolators, and general manipulators [13–23].

A number of statically balanced compliant mechanisms can also be found in literature. These mechanisms are focused on the fundamental underlying principle where a mass or point of interest is balanced to lower the actuation load, while keeping the benefits of the compliant design. It is possible to use this method to design statically balanced compliant joints, which can be achieved using conventional, external springs [24] or by replacing them with external flexures [25]. These rotational joints have 1 degree-of-freedom (DoF) with an operational range of approximately $1.4 [rad]$, which is considered large for compliant mechanisms. Another widely explored approach is the static balancing of a 1-DoF four-bar mechanism, for which several methods are available. The first method uses superposition to counteract the constraining leaf flexures with preloaded leaf springs [26–28]. A constant load domain is created because the total stiffness is reduced to zero, however the actuation range is small compared to the size of the mechanism. The other method does not require the use of external stabilizing mechanism, but rather makes use of preload inside the joints of the mechanism. This comes in the form of using conventional rotational springs [29] or leaf flexures [30, 31]. By optimizing the potential energy for the preloaded position and the stiffness of joints, it is possible to create statically balancing in these 1 DoF systems over a large range.

However, these statically balanced mechanisms discussed are generally limited to 1 DoF, as their structural compliant constraints make them simple to manage and control. A drawback of these structures is the restricted motion of the point of interest, often resulting in unwanted movements, like a rotational motion when only linear movement is desired. Furthermore, the limited rotation range of compliant flexures combined with this drawback often result in a relatively small actuation range compared to the size of the mechanism. Expanding the mechanism into a multi-DoF system offers a more adaptable design approach, allowing the end effector to achieve the precise desired movement. With additional degrees of freedom, the system becomes less constrained, enabling a broader range of motion and greater actuation possibilities, which can enhance the mechanism’s overall functionality and application flexibility.

The goal of this paper was to optimize and prototype a multi-DoF statically balanced compliant mechanism that is restricted in the 2-dimensional plane. The method is based on the principle of preloading the joints without the use of external springs, as previous studies have shown a great ability for a large actuation domain. The intended requirements for the mechanism were as follows:

Requirements:

1. The y-movement of the EE has been set to a range of $50 < y < 150 [mm]$. The domain does not begin at $y = 0$, as this allows for a better design flexibility.
2. The rotational movement of the EE has been set to $-0.5 < \theta < 0.5 [rad]$.

These requirements add up to a actuation domain consisting of a grid of points of all the possible combinations of y and ϕ . A visualisation of the EE movement has been given in Figure 1. Actuators will provide the necessary stiffness and control to manipulate the end effector (EE). Preliminary tests demonstrated that having a mechanism with these two DoF is difficult to realize, but by symmetrically preloading a 3 DoF linkage along the y-axis (Figure 2) keeps the end effector at a neutral x-position of 0. Therefore, the model uses input variables y and θ as DoF and x will be set to 0 and not taken into account.

The paper is organized as follows. In section 2, a new methodology is introduced for designing statically balanced multi-DoF compliant mechanisms. This methodology is demonstrated through a case study specifically designed for this purpose. A design vector is defined which will be optimized in the end. Utilizing inverse kinematics, the model is completely constrained after which the potential energy equation the outline of the optimization algorithm are introduced. In section 3, both the hypothesis and an alternative mechanism are modeled and optimized. The model of the chosen mechanism is then translated into a physical prototype, detailed in section 4. How the experimental validation is defined and how these experimental results will be produced is discussed in section 5 and section 6, respectively. The paper concludes with a discussion of the overall process and findings (section 7), followed by the conclusion in section 8.

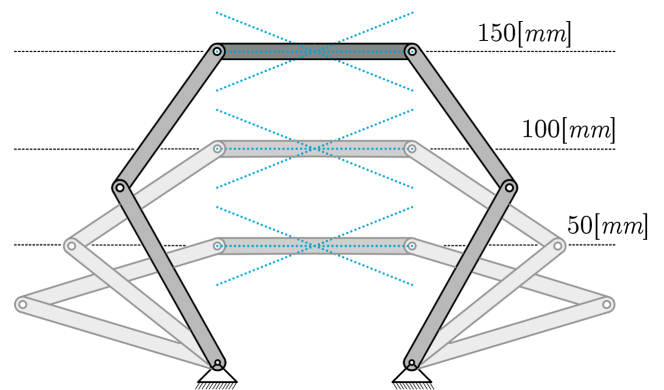


FIGURE 1: Visualisation of the domain, where the end effector can move over a range of $50 < y < 150 [mm]$ and rotate around its axis from $-0.5 < \theta < 0.5 [rad]$.

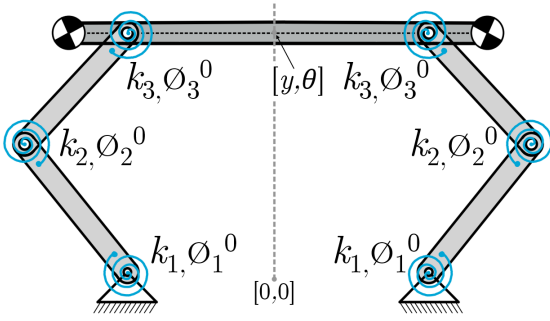


FIGURE 2: Visualization of the case study, showing the mechanism preloaded symmetrically over the grey vertical line and theoretical fixation at $x = 0$.

2 Design Methodology

A new design methodology has been developed for the application of the statically balancing characteristic in a multi-DoF mechanism. To maintain static balance, the system's potential energy must remain constant throughout all the possible combinations of the input variables y and θ . This can be achieved by ensuring the derivative of the system's potential energy towards both DoF is zero across the whole domain. The potential energy equation of the mechanism is set up using Pseudo-Rigid-Body Modelling (PRBM), where the flexible members are modelled as revolute joints and torsional springs. The potential energy does not have to be only dependent on rotational stiffness, but can also incorporate masses as compensation principles which creates another design dimension that could improve the performance.

The general steps in this design methodology are explained using the case study visualized in Figure 2. It can be seen that the preload angles and the joint stiffnesses are symmetrically designed over the y -axis to keep the end effector located in a neutral x -position. The potential energy equation of this system is dependent on the input variables (y and θ) and the design parameters, but the design process starts by converting the proposed case study into a PRBM. The case study is expanded by adding spiral springs to represent the torsional stiffness of each joint and establishing the fundamental components. Figure 3 illustrates the mechanism's geometry and parameters that will be used. The length of all the members have been set to a fixed values of $L_1 = L_2 = L_{EE} = 100[mm]$.

The design parameters are the free variables that will be optimized to influence the mechanism's functionality and achieve static balance. These parameters are captured in the design vector Ω , which can be expressed as:

$$\Omega = [k_1 \ k_2 \ k_3 \ \phi_1^0 \ \phi_2^0 \ \phi_3^0 \ x_a \ y_a \ \delta \ m], \quad (1)$$

where k_i are the stiffness of their respective joint in $[Nm/rad]$ and ϕ_i^0 are all the preloads for that corresponding flexure in $[rad]$. These are the most crucial design parameters. The re-

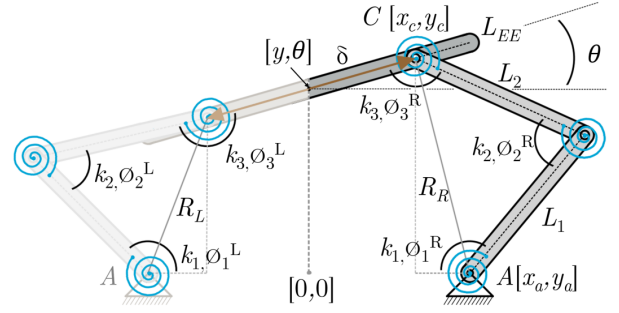


FIGURE 3: The case study configuration where all the parameters in design vector Ω and the other variables are visualized.

maining parameters describe the geometry of the mechanism, with (x_a, y_a) being the coordinates of the rigid connection point A, δ is a scaling factor determining the connection location on the end effector and m describes the added masses. Any subset of parameters within the design vector can be selected for optimization, while the remaining parameters will be treated as fixed. Additionally, it is feasible to introduce extra rigid connection points, such as (x_b, y_b) , if additional compensating beams are incorporated into the end effector.

Ω is used alongside the input parameters $[y, \theta]$ to fully constrain the entire mechanism. However, the relationship between the parameters and the energy curve remains unknown. Therefore, it is crucial to determine the rotational displacement of each joint at every point within the end effector's domain. This is done using inverse kinematics [32] where all the rotations in the mechanism are calculated according to the end effector's input movement. These displacements are described by ϕ_i^L and ϕ_i^R , where $i = \{1, 2, 3\}$ and L/R describes the side of the mechanism.

Right Side: The first step is to described the connection points of the legs to the end effector, which are the coordinates of point C (x_c^R, y_c^R) . They are described by:

$$x_c^R = x + \delta \cdot L_{EE} \cdot \cos(\theta), \quad (2)$$

$$y_c^R = y + \delta \cdot L_{EE} \cdot \sin(\theta). \quad (3)$$

With these coordinates known, a new length R_R is setup. This is the distance between rigid connection point A and attachment point C.

$$R_R = \sqrt{(y_c^R - y_a)^2 + (x_c^R - x_a)^2} \quad (4)$$

With all lengths and coordinates known, the rotational displacements at each joint is determined using the law of cosines and trigonometry. The rotations have the following form:

$$\phi_1^R = \text{acos}\left(\frac{L_1^2 + R_R^2 - L_2^2}{2L_1R_R}\right) + \text{atan}\left(\frac{y_c^R - y_a}{x_c^R - x_a}\right) \quad (5)$$

$$\phi_2^R = \text{acos}\left(\frac{L_1^2 + L_2^2 - R_R^2}{2L_1L_2}\right) \quad (6)$$

$$\phi_3^R = \text{acos}\left(\frac{L_2^2 + R_R^2 - L_1^2}{2L_2R_R}\right) + \text{atan}\left(\frac{x_c^R - x_a}{y_c^R - y_a}\right) + S_R \quad (7)$$

where $S_R = \frac{1}{2}\pi - \theta$ which is a term added to describe the angle between link 2 and the end effector.

Left Side: The left side of the mechanism uses the same equations as Eq. 7 to 9, however the terms x_c^L , y_c^L and S^L are slightly different to their mirrored counterparts. This can all be retrieved from evaluating the mechanism using trigonometry and have the form:

$$x_c^L = x + \delta \cdot L_{EE} \cdot \cos(\theta). \quad (8)$$

$$y_c^L = y - \delta \cdot L_{EE} \cdot \sin(\theta), \quad (9)$$

which add up to the final equations being:

$$\phi_1^L = \text{acos}\left(\frac{L_1^2 + R_L^2 - L_2^2}{2L_1R_L}\right) + \text{atan}\left(\frac{y_c^L - y_a}{x_c^L - x_a}\right) \quad (10)$$

$$\phi_2^L = \text{acos}\left(\frac{L_1^2 + L_2^2 - R_L^2}{2L_1L_2}\right) \quad (11)$$

$$\phi_3^L = \text{acos}\left(\frac{L_2^2 + R_L^2 - L_1^2}{2L_2R_L}\right) + \text{atan}\left(\frac{x_c^L - x_a}{y_c^L - y_a}\right) + S_L \quad (12)$$

where $S_R = \frac{1}{2}\pi - \theta$.

The total potential energy of the system (U_{tot}) is primarily composed of elastic potential energy, derived from the torsional stiffness of the joints, but also gravitational potential energy resulting from the added masses. Using Eq. 4 to 16, the design vector Ω and the domain parameters $[y, \theta]$, the total potential energy can be described and expanded to the following form:

$$\begin{aligned} U_{tot} = & \frac{1}{2} \cdot k_1 \cdot ((\phi_1^L - \phi_1^0)^2 + (\phi_1^R - \phi_1^0)^2) + \dots \\ & \frac{1}{2} \cdot k_2 \cdot ((\phi_2^L - \phi_2^0)^2 + (\phi_2^R - \phi_2^0)^2) + \dots \\ & \frac{1}{2} \cdot k_3 \cdot ((\phi_3^L - \phi_3^0)^2 + (\phi_3^R - \phi_3^0)^2) + \dots \\ & m \cdot g \cdot (y_c^L + y_c^R) \end{aligned} \quad (13)$$

2.1 Optimization Objective

Statically balancing refers to a condition where a mechanical system or object remains in equilibrium under static conditions, meaning no external forces or torques are causing it to move or rotate. In other words, all forces and moments acting on the system are balanced, and the system stays in a stable position without requiring continuous external input or correction.

As there are 2 DoF in the actuation domain, the derivative to both variables need to be optimized. Deriving the potential energy towards variable y results in

$$F = \frac{\partial U_{tot}}{\partial y}(\Omega, y, \theta), \quad (14)$$

where F is the notation for the force equation that is located on the end effector. Taking the derivative with respect to θ results in

$$M = \frac{\partial U_{tot}}{\partial \theta}(\Omega, y, \theta), \quad (15)$$

where M is the notation for the moment located on the end effector to rotate it to a certain θ position. Both these equations are implemented in Matlab with a multi-objective genetic algorithm using the function 'gamultiobj' to create a constrained nonlinear optimization problem. The goal of this optimization is to determine the values of the variables in design vector Ω . However, filling in the equations for F and M straight into the optimization objective is not possible due to 2 reasons:

1. As this is a multi-objective optimisation problem, the derivatives need to be normalized in order for them to be comparable by the genetic algorithm. This is done using Min-Max Normalization.
2. The input over which statically balancing is being created is a whole domain of points, so the Root-Mean-Square (RMS) needs to be taken to get a correct formulation of the objective.

The normalized versions of Equations 14 and 15 are used in the RMS for every combination of y and θ . These equations can be utilized as objective functions for the optimization problem. By incorporating all the variables within the design vector Ω , the optimization problem can be solved. The problem is subjected to:

$$\begin{aligned} \text{find } & \mathbf{k} = [k_i], \quad \phi^0 = [\phi_i^0], \quad \mathbf{x} = [x_i], \\ & \mathbf{y} = [y_i], \quad \delta = [\delta_i], \quad \mathbf{m} = [m_i] \\ \text{to minimize } & f(\Omega) = \{f_F(\Omega), f_M(\Omega)\}, \\ \text{where } & \Omega = \{\mathbf{k}, \phi^0, \mathbf{x}, \mathbf{y}, \delta, \mathbf{m}\} \\ \text{subjected to } & G_1 \equiv k_i \in [k_{min}, k_{max}], \quad i = \{1, 2, 3\}; \\ & G_2 \equiv \phi_i \in [\phi_i^{min}, \phi_i^{max}], \quad i = \{1, 2, 3\}; \\ & G_3 \equiv x_i \in [x_{min}, x_{max}], \quad i = \{a, b\}; \\ & G_4 \equiv y_i \in [y_{min}, y_{max}], \quad i = \{a, b\}; \\ & G_5 \equiv \delta_i \in [\delta_{min}, \delta_{max}], \quad i = \{1, 2\}; \\ & G_6 \equiv m_i \in [m_{min}, m_{max}], \quad i = \{1, 2\}; \end{aligned}$$

where f_F and f_M are the normalized objective functions for the force and moment respectively and G_i describes the constraints for the objective.

Constraints G_3 to G_6 are non-critical constraints, as they define the mechanism's geometry and can therefore be easily configured. Constraints G_3 and G_4 have been set to

$$G_3 \equiv x_i \in [50, 100] \text{ [mm]}, \quad i = \{a, b\};$$

$$G_4 \equiv y_i \in [0, 50] \text{ [mm]}, \quad i = \{1, 2\};$$

to give the arms of the end effector rooms to be optimized while keeping the size and shape of the mechanism in mind. The weight of the links are assumed to be zero and the stiffness matrix is considered constant over the whole actuation domain. Constraint G_5 has been set to $\delta \in [0.3 : 1]$ as a scaling factor for the attachment points of the end effector and G_6 has been set to $m \in [0 : 0.1][kg]$.

Constraints G_1 and G_2 are more sensitive and need more precaution setting them up. Constraint G_1 takes the geometry of the flexure in mind, which has been set at a fixed length of $L_f = 20[mm]$ and a thickness of $0.8[mm]$. Using Equation 19, k_{min} was calculated and an estimation of k_{max} was made. These constraints have been set to a value of

$$k_{min} = 0.02 \frac{Nm}{rad} \quad \text{and} \quad k_{max} = 0.1 \frac{Nm}{rad}.$$

Constraint G_2 cannot be predetermined as it depends not only on the mechanism's geometry (x , y , and δ), but also on the maximum rotation angle of each joint. The ability of statically balancing heavily relies on the magnitude potential energy within the system, which is higher the larger the rotation of the flexure. Taking non-linearities into account, Howell et al. [33] reports a flexure rotation limit of 1.344 [rad] (77 [deg]) as a general rule of thumb for designing flexures. Consequently, the boundary constraints of the problem must be updated between optimization runs and cannot be fixed in advance, otherwise the rotations will exceed this limit. Initially, the optimization parameters are set, and the boundaries of the preload constraint are defined for a given configuration. During the first iteration, the preload boundary conditions are updated based on the (x, y)-values the optimizer converges to. At the end of this iteration, these (x, y)-values are fixed, and the second iteration begins. This iteration follows the same procedure, but results in the fixation of values for δ and m . Finally, the last run yields the stiffness and preload values required for static balancing. This process is outlined in the flowchart shown in Figure 4.

3 Evaluation of Optimized Designs

The design methodology can be applied to various configurations and mechanisms, with two specific configurations highlighted for achieving a display of static balancing. The first example investigates the case study and its ability to create static balancing. The second mechanism removes the added masses, but uses extra linkage legs to balance out the existing structure. This involves adding terms to the design vector, but the general use of Inverse Kinematics remains as described.

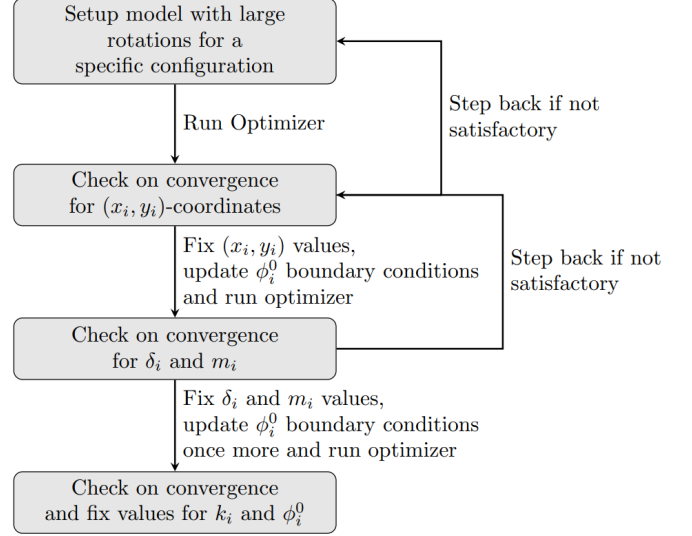


FIGURE 4: A flowchart explaining the steps taken in the optimization strategy.

3.1 Case Study

The mechanism proposed in the case study serves as a gravity balancer, which is advantageous because the mechanism functions like a traditional spring due to its shape. This means that the mechanism provides a general upward force for any position or preload. By adding masses, this upward momentum can be offset to achieve a net zero force on the end effector across the actuation domain. This leads to the following design vector:

$$\Omega = [k_1 \quad k_2 \quad k_3 \quad \phi_1^0 \quad \phi_2^0 \quad \phi_3^0 \quad x_a \quad y_a \quad \delta \quad m]$$

Running the optimizer will yield a unique combination of parameters in the design vector that provides the optimal static balancing performance.

The mechanism has converged towards a (x_a, y_a)-position at $(66, 0)[mm]$ after which it showed convergence for scaling factor $\delta = 0.4263$ and a mass of $m = 0.0265[kg]$. Using these values for the optimizer results in the most optimal situation where k and ϕ are:

	Stiffnesses [$\frac{Nm}{rad}$]	Preloads [rad]
k_1	0.0776	ϕ_1^0 1.45
k_2	0.0277	ϕ_2^0 1.36
k_3	0.0159	ϕ_3^0 2.77

TABLE 1: The final values of the parameters for the best configuration in the hypothesis.

which finalizes all the parameters in the design vector.

The results for the external force are plotted in Figure 5. As can be seen the force to keep the end effector in a certain y-position fluctuates from $-0.2 [N]$ to $0.5 [N]$ for multiple θ positions. These results are compared to the same mechanism without preloads but with equal stiffnesses, to highlight the working principle of preloading. In comparison to the unloaded mechanism, this comes down to a peak force reduction of around 80%.

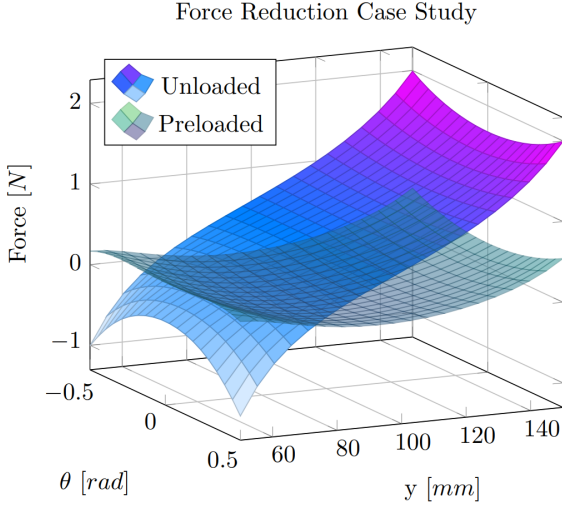


FIGURE 5: Surf plot over the whole actuation domain for the required external force to keep the end effector at a certain (y, θ) -position in the hypothesis.

As for the moment, the peak reduction is around 50%. The required moment to keep the end effector at its certain position is around -0.05 to $0.05 [Nm/rad]$, however this differs for different y-positions. The unloaded mechanism requires a moment from around -0.1 to $0.1 [Nm/rad]$. The plot for the moment can be found in Appendix D.

3.2 Compensated Beams Mechanism

The second mechanism that has been explored removes the masses and replaces them with additional linkage legs, drawing inspiration from Rijff et al. [29]. The concept is that by adding more links in a specific configuration, the additional rotational displacements counteract the existing joints, creating more opportunities for statically balancing. This necessitates an expansion of the design vector to:

$$\Omega = [k_1 \ k_2 \ k_3 \ \phi_1^0 \ \phi_2^0 \ \phi_3^0 \ x_a \ y_a \ \delta_1 \ \dots \\ k_4 \ k_5 \ k_6 \ \phi_4^0 \ \phi_5^0 \ \phi_6^0 \ x_b \ y_b \ \delta_2]$$

where the bottom row contains the new parameters of the added links, as can be seen in Figure 6. After this, the same principle is used as the gravity balancer which makes use of the flowchart provided.

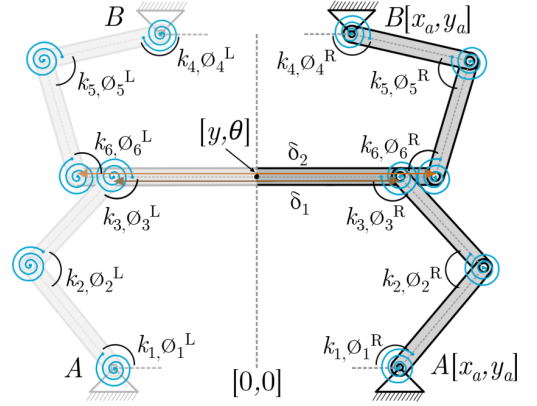


FIGURE 6: Visualisation of the expansion for the compensated beams mechanism. While the joints are still mirrored over the y-axis, the new linkages have their own respective preload and stiffness.

The optimizer has been run multiple times with all design variables available, while the preload domain has to be adjusted between runs. After three iterations, it became evident that the best results were achieved with a fully symmetric model, where the x-x and y-y planes are mirrored. This means that $x_a = x_b$, $y_a = y_b$, $\delta_1 = \delta_2$, $k_{1-3} = k_{4-6}$ and $\phi_{1-3}^0 = \phi_{4-6}^0$ will be fixed for the subsequent runs. The next iterations is performed with the updated design vector until the objective converged around optimized values for x_a , y_a , and δ_1 . These final values are $x = 0.7 [mm]$, $y = 0 [mm]$, and $\delta = 0.35$, which will remain fixed for the final optimization steps. First, the boundary conditions for the preloads are updated to:

$$\phi_i \in \begin{bmatrix} \phi_1^{min} & \phi_2^{min} & \phi_3^{min} \\ \phi_1^{max} & \phi_2^{max} & \phi_3^{max} \end{bmatrix} = \begin{bmatrix} 0.866 & 0.716 & 2.906 \\ 3.224 & 1.864 & 3.194 \end{bmatrix}$$

This is done by checking the rotational displacements over the whole domain, write down the smallest and largest rotational values and add/subtract the rotation limit. In the last iteration, the best possible configuration was found with the following parameters:

Stiffnesses $[\frac{Nm}{rad}]$	Preloads $[rad]$
k_1	ϕ_1^0 3.01
k_2	ϕ_2^0 1.82
k_3	ϕ_3^0 0.91

TABLE 2: The final values of the parameters for the best configuration the compensated beams mechanism.

Using the values in the final design vector, the necessary external force on the end effector over the actuation domain is calculated and plotted in the surf plot in Figure 7. As can be seen, this external force stays roughly within ± 0.05 [N] which is a reduction of force around 97.5% at the outermost positions.

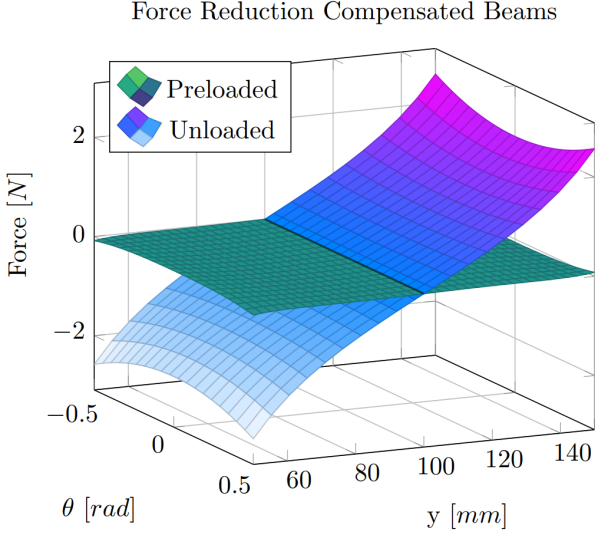


FIGURE 7: Surf plot over the whole actuation domain for the required external force to keep the end effector at a certain (y, θ) -position for the compensated beams mechanism.

Currently, the moment reduction is approximately 95%, as the required torque to maintain the end effector in position is around ± 0.0025 [Nm/rad] across most of the actuation range compared to the required torque of around ± 0.1 [Nm/rad] for the unloaded mechanism. At the outer positions, the theoretical reduction is slightly lower but remains above 90%. A plot illustrating the moment necessary in the unloaded mechanism can be found in Appendix D.

3.3 Case Study vs. Compensated Beams

While the gravity balancer effectively reduces external loads, introducing additional compensating beams in a novel configuration achieves a performance comparable to the established results for 1-DoF systems, with reductions exceeding 90%. This approach not only enhances load balancing but also offers flexibility in the integration of the end effector, opening up diverse possibilities for future applications. Due to these advantages, the following sections of the paper will concentrate on the compensated beam mechanism, examining its design, performance, and potential uses in greater detail.

4 Flexure Arm Design and Prototyping

Selecting the dimensions and material of the flexures are two factors that are closely intertwined due to their nonlinear behavior and the stresses induced during large deflections. The maximum stress in a rectangular beam with a constant cross-section, subjected to a moment M at its tip, is given by:

$$\sigma_{max} = \frac{Mw}{2I} \quad (16)$$

where I is the second moment of area of the cross-section, and w [mm] is the width of the flexure. Under bending stresses, it is assumed that for large deflections, the solution to the Bernoulli-Euler equations under pure bending is given by:

$$M = \frac{\alpha EI}{L_f} \quad (17)$$

where α represents the rotation limit of 1.344 radians, E denotes the Young's modulus of the material, and L_f is the length of the flexure. By adding Equation 16 and Equation 17, the following expression is obtained:

$$\sigma_{max} = \frac{\alpha Ew}{2L_f} \quad (18)$$

where the combination of the length and width of the flexure can be compared to the Young's Modulus and yield strength which make up the material.

Howell [34] and Gallego [30] propose applying a 10:1 ratio to maintain the functionality of the flexures while keeping their lengths in proportion with the link dimensions. Given that the links of the mechanism are 100 [mm] long, a flexure length of 10 [mm] is appropriate. However, since two links are connected by the same flexure, the total length of a flexure will be $L_f = 20$ [mm].

Producing the flexure of the same material as the links offers several advantages, including easier assembly of the mechanism, reduced risk of production errors during flexure installation, and the ability to create quick prototypes. Consequently, the flexures will also be 3D printed. The available FDM printer has a standard nozzle size of 0.4 [mm], which, due to the nature of the layer paths, limits the flexure to a minimum width of $w = 0.8$ [mm]. Since increasing the flexure thickness would raise the stress at the joint, it has been decided to fix this width for all flexures.

The 3D printer that has been used for this project is a Bambulab P1S printer that has the ability to print the following, conventional materials:

PLA: $E = 3.15$ [GPa] $\sigma_y = 60$ [MPa]

ABS: $E = 2.1$ [GPa] $\sigma_y = 47.5$ [MPa]

PETG: $E = 2.0$ [GPa] $\sigma_y = 50$ [MPa]

TPU: $E = 0.05$ [GPa] $\sigma_y = 15$ [MPa]

Filling in these material properties in Equation 18 indicates that PETG and TPU are the only two viable options for this application. While TPU meets the requirements, its flexibility results in high viscoelasticity and very low stiffness. Although the flexure will not fail under these conditions, it will not return to its printed position quickly or with high force. Therefore, PETG is selected as the material for this project.

The next step was to calculate and fixate the height of the flexures using,

$$k = \frac{EI}{L_f} \rightarrow w = \frac{12kL_f}{Et^3} \quad (19)$$

where k is the stiffness of the flexure, $L = 20$ [mm] is the fixed length, $E = 2.0$ [GPa] is the Young's modulus, and $t = 0.8$ [mm] is the thickness of the flexure. The height of the flexure determines its stiffness, which is why the boundary condition is set at $k_{min} = 0.02$ [Nm/rad], corresponding to a minimum flexure height of approximately 4.6 [mm]. The mechanism would otherwise become too flimsy. To prevent the mechanism from becoming too bulky, a maximum limit of $k_{max} = 0.1$ [Nm/rad] or $w = 23.4$ [mm] has been established.

The width of the flexure has to be designed in increments of 0.2 [mm] as this is the designated layer height step the printer is capable to print. This is why the optimized stiffnesses from Table 2 cannot be exactly matched to a certain height and have to be rounded up- or downwards depending on the layer height. This creates the following dimensions and final stiffnesses:

New Stiffness [$\frac{Nm}{rad}$]	Dimensions [mm]	
k_1	0.02048	20x4.80x0.8
k_2	0.05376	20x12.6x0.8
k_3	0.05547	20x13.0x0.8

TABLE 3: Final stiffnesses and dimensions of the flexures inside the mechanism.

With the geometry fixed and the material selected, the focus now shifts to designing the compliant linkage that will replace the revolute joints in the PRBM. Since the mechanism is symmetrical about both axes, it suffices to examine just one of the four arms to explain the transition from the PRBM to the mechanism. Figure 8 provides a visualization in which the preload is clearly shown in PRBM form. Link 1 must be preloaded along the striped line while the end effector remains in position. If this is done for all four legs, the mechanism will be fully assembled.

However, this illustration still lacks the compliant flexures in the design, meaning the PRBM needs to be translated into a compliant mechanisms. As known, a compliant flexure can be modelled as a revolute joint with a rotational joint attached. This

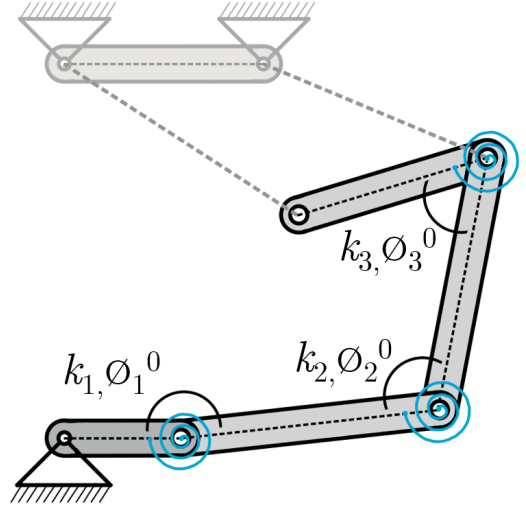


FIGURE 8: Visualisation of the PRBM where the manufacturing position is taken in mind. The dotted lines describe the displacement necessary to apply the correct preload.

modelling also works reversed. It is stated that during the translation, the traditional revolute joint can be placed on the midpoint of the flexure. This means that the center of the flexure will lie on the joint in the PRBM. The angle at which the flexure is implemented is not critical, however for simplicity in design it has been determined that the flexure will be positioned perpendicular to the midpoint line between the two connected members. As a result, the lengths of the links will be changed. An illustration of the flexures in the compliant mechanism together with the new dimensions of the links has been given in Figure 9.

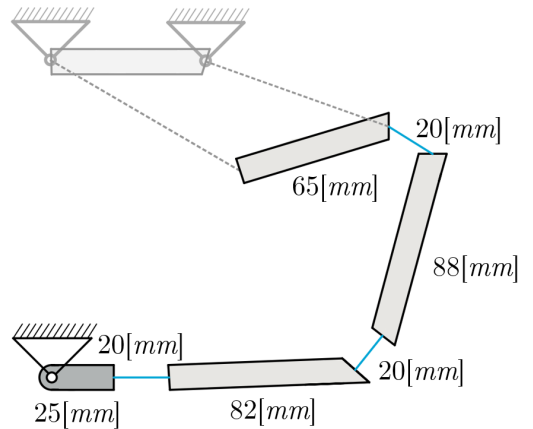


FIGURE 9: The translation from PRBM to compliant design involves replacing the joints with the chosen flexures on the correct position. This changes the lengths of the rigid members.

The flexure arms are printed separately and without supports, to keep it simple and reduce printing errors (Figure 10). Assembly is done by connecting four of these flexures to each other using the end effector. Preload is applied through a designated baseplate, where link 1 of all the arms will be moved to its preloaded position. The same approach will be applied to the non-preloaded mechanism. In this case, the design will not involve any preloads and the mechanism can directly be placed on the baseplate.

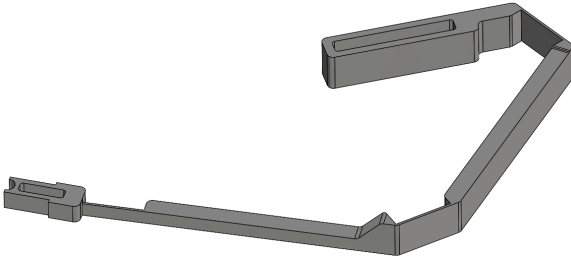


FIGURE 10: CAD Design of the flexure arm. The change in height over the length of the arm causes the joints to have various stiffnesses.

5 Experimental validation

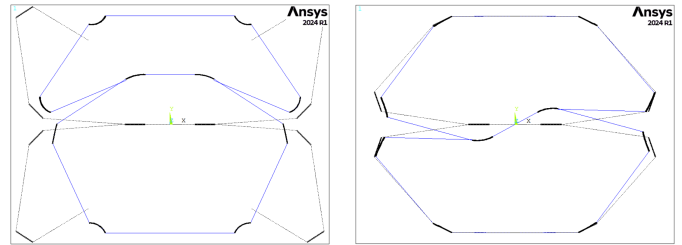
The predicated function of the mechanism was validated using 2 methods. The first is through Finite Element Analysis (FEA) using the program ANSYS. Ansys is a powerful simulation software used in various engineering fields. One of its key features is its FEA capabilities, which allows users to analyse structures under various loading conditions. For this project it is especially useful as Ansys is highly capable of analysing nonlinear deformations. Ansys will be utilized to capture the nonlinearities in the mechanism that are not accounted for in the PRBM and therefore will create a better understanding of the mechanism. The second method is physical testing. The best way to test the characteristics of a mechanism is through prototyping and testing, it will give the best results and it is also easily processed. Laying the results of Ansys and testing next to each other, the PRBM and the accuracy of the model can be confirmed.

5.1 Ansys APDL

Ansys APDL has different element types that are predefined sets of finite elements that define the behavior of structures under various physical conditions. For the flexures, BEAM188 elements are used. This is a 3 Dimension, 2 Node beam element that has 6 DoF at each node. This element is based on Timoshenko beam theory, which includes shear deformation effects and makes sure for precise determination of the mechanism. For simplicity, the links between the flexure are assumed to be rigid utilizing the MPC186 element.

The mechanism was built in Ansys APDL by describing the coordinates of all the end points of the flexures and links. These coordinates describe keypoints in between which lines are drawn with the respective element type, material characteristics and dimensions after which they are meshed for simulations. This is done in the preprocessor of which visualisations can be found in Figure 11 in grey. In the simulation step for the force on the end effector, the keypoints of the preload link are first shifted to their preloaded positions. After this, in the second timestep, the end effector keypoints are moved to $+50[mm]$ and then to $-50[mm]$. In the post-processor, the force that is needed to facilitate this movement can be extracted and plotted.

For the moment simulations, the preprocessing steps are repeated after which the end effector will be rotated to $-0.5[rad]$ and $0.5[rad]$ in the simulation step. As a benchmark, the same tests will be performed for the unloaded mechanism.



(a) Preloaded mechanism with vertical displacement.

(b) Unloaded mechanism with rotational displacement.

FIGURE 11: Screenshots for the Ansys software where the mechanism is modelled and actuated (blue). In picture (a) the manufactured shape of the arms can be seen in grey.

5.2 Physical Testing

The printed mechanism fully assembled and preloaded on the baseplate is placed in the test setup (Figure 12). The test setup makes use of a PI linear stage with a maximum stroke of $100[mm]$ to push and pull on the end effector. The mechanism itself is mounted on a $25 \times 25[mm]$ profile, which is securely fastened to the breadboard with the linear stage. For the unloaded mechanism and the moment measurement on the preloaded mechanism, a Futek LSB205 FSH04785 - 44.5N force sensor is used to measure the external loads. However, the measurement resolution of this sensor is too large to measure the curve of the force located on the preloaded mechanism. Therefore the Futek LSB200 FSH03868 - 0.2N sensor has been used to complete this measurement. These sensors are rigidly attached to the custom-designed end effector, allowing the linear stage to both push and pull on the mechanism. For the neutral position of the mechanism and simulations, at $y = 100[mm]$, the linear stage has been set to 0.

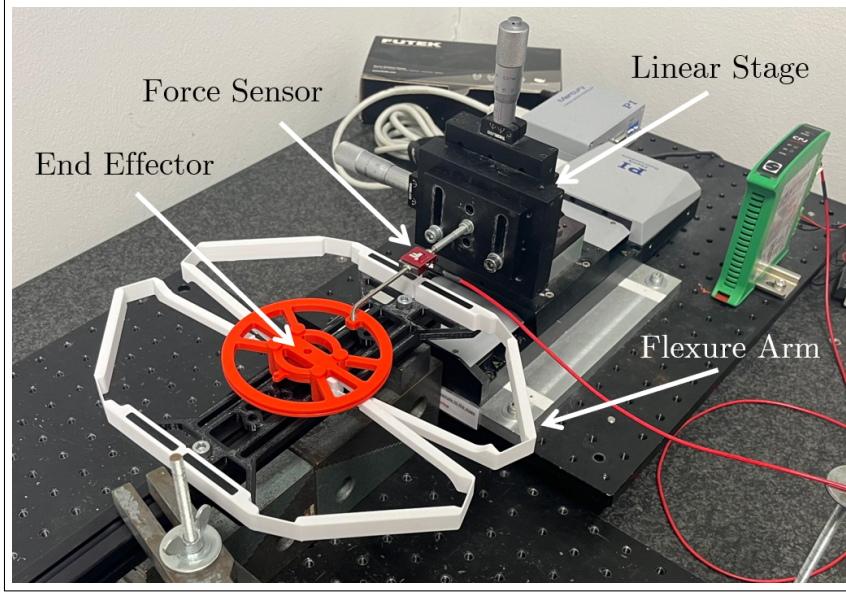


FIGURE 12: *Compensated beams mechanism inside the test setup for the force-displacement measurement. The end effector (red) is connected to the sensor and the flexure arms (white) fixates the mechanism to the baseplate. For the moment measurement, a fishing wire is placed around the end effector, which can be seen in Appendix E*

6 Experimental Results

It is not feasible to measure and plot data across the entire actuation range, so only the two most critical measurements will be presented: the external force applied to the end effector while it is held in a horizontal position at $\theta = 0[\text{rad}]$, and the resulting moment on the end effector as it rotates around the neutral y-position at $y = 100[\text{mm}]$. The physical test results show some disturbances, and the mechanism exhibits hysteresis. Therefore, data fitting is necessary, and this is accomplished using a quadratic polynomial model. These tests have been conducted for both the unloaded and preloaded mechanisms to create a solid foundation for setting a benchmark and validating the test setup for errors that come with it

Force-displacement measurements

Rotation of the end effector is undesired when it comes to measuring a pure force on the mechanism. That is why safety pins in the end effector ensure that no rotational motion can occur during testing, closely following the isolated movement that is possible in the Ansys software. The test will begin by moving the linear stage to the $+50[\text{mm}]$ position, followed by movement to the $-50[\text{mm}]$ position. After returning the end effector to its neutral position, the test is complete. This process will be repeated five times to assess repeatability, nonlinearities, and plastic-elastic behavior in the mechanism. In section 6, the recorded data is compared with the PRBM and Ansys results to validate the accuracy of the simulation.

Torque-rotation measurements

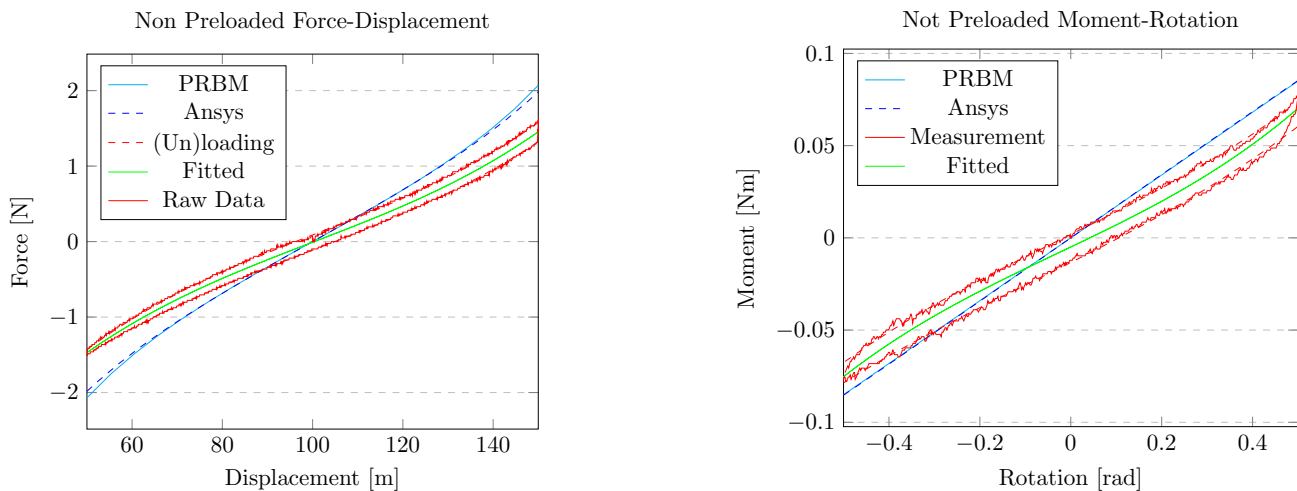
Measuring the moment using a linear stage is not as straightforward as measuring the force. Here, the force sensor is connected to the end effector by routing fishing wire around the circular shape ($r = 50[\text{mm}]$) of the end effector, with on the other side a counterweight. The counterweight provides a load in the opposite direction which stabilizes the linear motion into a rotation. The contribution of the counterweight needs to be subtracted from the measured force values. It is then necessary to convert the rotational motion into a linear translation, which will be achieved by using this relationship:

$$y = \frac{2\pi r}{2\pi} \cdot \theta = \frac{2\pi \cdot 50[\text{mm}]}{2\pi} \cdot 0.5 = 25[\text{mm}] \quad (20)$$

where y represents the movement of the linear stage. It has been calculated that the stage needs to travel from $-25[\text{mm}]$ to $+25[\text{mm}]$ to rotate the end effector between $-0.5[\text{rad}]$ and $0.5[\text{rad}]$. Meanwhile, the end effector is fixed on $y = 100[\text{mm}]$, removing x- and y-displacements. The measurement will be conducted five times, after which the data needs to be converted from force to moment using:

$$M = F \cdot r \quad (21)$$

Here, F represents the measured force, and r is the radius of the end effector. The linear displacement will be converted back into radians using Equation 20, ensuring that the measured data can correctly be compared with the results from the PRBM and the Ansys simulations.



(a) Force-Displacement curve of the unloaded mechanism with the end effector kept at a horizontal position of $\theta = 0[\text{rad}]$.

(b) Moment-Rotation curve of the unloaded mechanism at the neutral position of $y = 100[\text{mm}]$.

FIGURE 13: The PRBM model, Ansys simulations and measurements of the unloaded mechanism plotted against each other for both the external force and moment required. The light blue line highlights the PRBM and the dashed blue line represents the Ansys simulations. The physical measurements are shown in red, and due to hysteresis the data has to be fitted which is shown in green.

7 Discussion

Unloaded Mechanism Visualised in Figure 17, it can be seen that the alignment between the Ansys simulations and the PRBM model is near identical. This validates several aspects of the modelling process, including the correct implementation of the mechanism in Matlab, the correctness of the Ansys simulations but most importantly, the accurate conversion from the PRBM to a compliant model. With these consistencies being in the linear regime, it can be said that these simulations will also be reliable for the mechanism in the nonlinear domain. The physical results follow the general shape for both the force and moment simulations closely. Additionally, the closed loops observed in the measurements indicate that there is no plastic deformation in the material.

However, some inconsistencies between the simulated and measured values are visible. There is a slight mismatch in the magnitude of the load with differences of approximately $0.5[\text{N}]$ and $0.01[\text{Nm}/\text{rad}]$. These inconsistencies could arise from several factors. First, the Young's Modulus used in the simulations may deviate from the actual physical properties of the material. The PETG material, being 3D printed, is not homogeneous and the layer-based construction can introduce irregularities. Furthermore, the assumed rigid links in the model do not fully capture the slight bending occurring in the links of the physical model. The presence of hysteresis and data fluctuations could be explained by errors in the test setup, which mainly consist of added friction between the end effector, the baseplate and the fixation pin. Pulling and pushing motions cause for hysteresis due to changing load directions.

Preloaded Mechanism It is essential to start of by acknowledging that the measurements and simulations performed here deal with very low loads, on the order of $0.05[\text{N}]$ and $0.02[\text{Nm}/\text{rad}]$. As such, even small deviations can appear visually exaggerated, though their absolute magnitudes remain very small.

There is a notable difference between the PRBM and Ansys simulations, which is expected given the nonlinearities in the preloaded mechanism. Since the simulations of the unloaded mechanism align well with the respective models, it can confidently be stated that both the Ansys and PRBM simulations provide the correct behaviour of the preloaded system. This can also be concluded from the similarities in the shape of both the external force and moment plots (Figure 14). However, the expected external load is higher in both situations. In the force measurement it is not that prominent, having a peak moment raised from $0.03[\text{N}]$ to $0.06[\text{N}]$. The simulated moment is around 50 times higher than expected based on the PRBM model, suggesting that the nonlinear effects are more noticeable in this aspect of the mechanism's behavior. This result is somewhat unfavorable, as it reduces the mechanism's effectiveness in achieving static balance for the moment predictions.

For the *moment measurements*, there is a relatively large hysteresis curve. While not very problematic given the low magnitude of the moment involved, it still shows the influence of friction in the mechanism. The added friction is visualized by the difference between the actual and fitted data, distorting the measurements from their idealized values. The inability to zero out the sensor due to the friction and low actuation force causes

the fitted line not the cross through $(0, 0)$. The shape of the fitted line does not perfectly follow the curve of the ansys simulation, though it remains within reasonable range given the potential fabrication and test setup errors. The moment is around 45% higher than the Ansys simulations which comes down to a total moment reduction of 80%. This is drastically lower than the theoretical reduction.

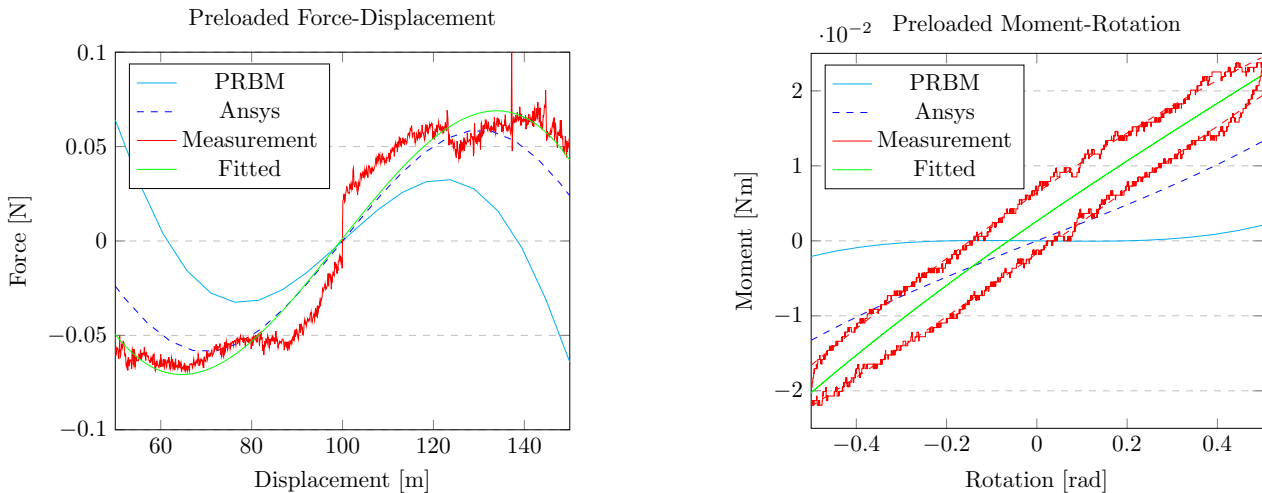
The *force measurements* follow, unlike the moment measurements, the force data of the Ansys simulations more closely. However, several notable disturbances were observed: first, a jump in force at the rest position $y = 100[mm]$, which can be explained due to the geometry of the test setup. The sensor's fixation point is located above the mechanism, so as the actuator pulls, a moment is created that leads to a slight shift of the end effector around the actuators mounting points. This causes the force to briefly shoot upwards. Similar effects can be seen at $y = 120[mm]$, where a small shift occurs due to increasing friction at that point. Lastly, a spike at $y = 138[mm]$ can be observed which happened due to the end effector shift back around the actuators mounting point due to the load direction change. The preloaded mechanism demonstrates an impressive reduction of 96% in force at peak force positions.

It has to be mentioned that there is no hysteresis curve visible for the force-displacement measurement of the preloaded mechanism. The return path of the linear stage has been removed from the plot, because during multiple tests the sensor returned distorted values. This happened because the friction and errors accompanying the return path overcame the extremely low actuation force required for movement.

7.1 Evaluation of the Mechanism

The general working principle of the mechanism demonstrates considerable potential, especially in the versatility offered by the unit cell configurations. These configurations open up possibilities for various applications, such as vibration isolators and guiding systems. Although the mechanism may not be the most ideal solution for a robotic manipulator in its current form, it could still be implemented effectively, particularly if scaled down. By reducing the size, smaller actuators could be used and the overall weight of the system is reduced to a point where it could better support itself. Additionally, the stiffness of the joints could be increased to enhance out-of-plane stiffness, allowing the mechanism to better maintain its structural integrity.

However, there is a significant flaw in the design that affects its performance. During the preloading process, the flexures attached to the end effector undergo compression, which eventually leads to buckling. This issue is critical as it impacts the statically balancing characteristic of the mechanism, causing it to slowly change shape over time. The root of the problem lies in the preformed shape of the flexures, if they had been designed to remain under tension rather than compression, the issue would not arise. This flaw is not only relevant for multi-degree-of-freedom systems but could also affect simpler one-degree-of-freedom mechanisms, making it a fundamental design challenge that needs to be addressed.



(a) Force-Displacement curve of the preloaded mechanism with the end effector kept at a horizontal position of $\theta = 0[rad]$.

(b) Moment-Rotation curve of the preloaded mechanism at the neutral position of $y = 100[mm]$.

FIGURE 14: The PRBM model, Ansys simulations and measurements of the preloaded mechanism plotted against each other for both the external force and moment required. The light blue line highlights the PRBM and the dashed blue line represents the Ansys simulations. The physical measurements are shown in red, and due to hysteresis the data has to be fitted which is shown in green.

8 Conclusion

In conclusion, this paper successfully expanded the principles of statically balancing through preloading into the first multi-DoF application, demonstrating the potential for large actuation domains and reduced external actuation loads. While traditional systems typically utilize 1 DoF, this work showed that multi-DoF mechanisms can be achieved without external springs by harnessing the energy stored in compliant materials. The prototyped mechanism achieved a 96% reduction in force and an 80% reduction in moment, significantly increasing actuation efficiency. And while there were some areas where the physical performance diverges from the theoretical models, particularly with respect to moments and hysteresis due to friction and errors in the test setup, the overall performance of the mechanism validates the design approach. Preloading the joints in a compliant mechanism has proven to be applicable in multi-DoF systems where a higher energy efficiency is required. These findings provide a foundation for a new approach in the design and application of compliant mechanisms, such as vibration isolators, robotic manipulator and positioning stages.

8.1 Innovation

This work marks the first time a compliant statically balanced multi-DoF system has been both explored and successfully implemented. Historically, there has been little interest in such systems due to the inherent instability associated with multi-DoF linkages, which presented significant challenges in maintaining control and balance. However, this research expands on existing principles, extending them to a larger, more complex mechanism with a considerable range of motion relative to its overall size. A key achievement of this design is the successful static balancing of the translational degrees of freedom without relying on external springs or counterweights, a significant innovation in compliant mechanisms. The system offers advantages over the conventional fourbar mechanisms, remove the undesired coupled rotation or translation.

This design method also opens up new possibilities for existing compliant mechanisms, where preload integration could be utilized to considerably lower the actuation load, in opposite to complete static balance, as demonstrated in the case study. This methodology would contribute to the continued evolution of compliant mechanisms, pushing the boundaries of what can be achieved with flexible, lightweight systems.

8.2 Recommendation

This mechanism serves as a fundamental demonstration of what other techniques could be used with compliant mechanisms in contrast with the conventional approaches. One key recommendation would be to implement this mechanism in a real-world application, as its capabilities could be further validated and optimized in practical settings. Another area for exploration is making the rigid connection points dynamic, allowing the ex-

ternal load characteristics to be adjustable. This could lead to more versatile mechanisms where the behavior can be fine-tuned based on specific needs, improving its adaptability across various use cases. However, a new approach has to be taken to avoid buckling flexures in the mechanism. This could be done by constraining the optimizer to avoid flexures to be under straight compression.

Further improvements could involve implementing different compliant joints with a more complex profile enhancing the stiffness in the off-axis direction, but also scaling the mechanism could make it more suitable for tasks requiring smaller, more compact designs without sacrificing functionality. Together with this, changing the manufacturing technique could improve the stability of future iterations. For example, by constructing the mechanism out of homogeneous materials would likely lead to improved durability, precision, and performance. Lastly, implementing Shape Memory Alloys (SMAs) as compliant actuators has to be done to yield interesting insights into how the mechanism's stiffness could be increased for control.

REFERENCES

- [1] Herder, J., 2020. "Static and dynamic balancing of robots". In *Encyclopedia of Robotics*. Springer.
- [2] Essomba, T., 2021. "Design of a five-degrees of freedom statically balanced mechanism with multi-directional functionality". *Robotics*, **10**(1), p. 11.
- [3] Ebert-Uphoff, I., Gosselin, C. m. M., and Laliberte, T., 2000. "Static balancing of spatial parallel platform mechanisms—revisited". *J. Mech. Des.*, **122**(1), pp. 43–51.
- [4] Kuo, C.-H., and Lai, S.-J., 2016. "Design of a novel statically balanced mechanism for laparoscope holders with decoupled positioning and orientating manipulation". *Journal of Mechanisms and Robotics*, **8**(1), p. 015001.
- [5] Van Dorsser, W. D., Barents, R., Wisse, B. M., and Herder, J. L., 2007. "Gravity-balanced arm support with energy-free adjustment".
- [6] Takahashi, T., Zehnder, J., Okuno, H. G., Sugano, S., Coros, S., and Thomaszewski, B., 2019. "Computational design of statically balanced planar spring mechanisms". *IEEE Robotics and Automation Letters*, **4**(4), pp. 4438–4444.
- [7] Peng, Y., Bu, W., and Chen, J., 2022. "Design of the wearable spatial gravity balance mechanism". *Journal of Mechanisms and Robotics*, **14**(3), p. 031006.
- [8] Kang, L., Oh, S.-M., Kim, W., and Yi, B.-J., 2016. "Design of a new gravity balanced parallel mechanism with schönflies motion". *Proceedings of the Institution of Mechanical Engineers, Part C: Journal of Mechanical Engineering Science*, **230**(17), pp. 3111–3134.
- [9] Le Chau, N., Giang Le, H., and Dao, T.-P., 2021. "A gravity balance mechanism using compliant mechanism". In *Computational Intelligence Methods for Green Technology and*

- Sustainable Development: Proceedings of the International Conference GTSD2020 5, Springer, pp. 431–439.
- [10] Agrawal, S. K., and Fattah, A., 2004. “Gravity-balancing of spatial robotic manipulators”. *Mechanism and machine theory*, **39**(12), pp. 1331–1344.
- [11] Arakelian, V., 2016. “Gravity compensation in robotics”. *Advanced robotics*, **30**(2), pp. 79–96.
- [12] Robinson, G., and Davies, J. B. C., 1999. “Continuum robots-a state of the art”. In Proceedings 1999 IEEE international conference on robotics and automation (Cat. No. 99CH36288C), Vol. 4, IEEE, pp. 2849–2854.
- [13] Huang, H., Chen, Y., and Lv, Y., 2014. “A novel robot leg designed by compliant mechanism”. In Intelligent Robotics and Applications: 7th International Conference, ICIRA 2014, Guangzhou, China, December 17–20, 2014, Proceedings, Part I 7, Springer, pp. 204–213.
- [14] Megaro, V., Zehnder, J., Bächer, M., Coros, S., Gross, M. H., and Thomaszewski, B., 2017. “A computational design tool for compliant mechanisms.”. *ACM Trans. Graph.*, **36**(4), pp. 82–1.
- [15] Nguyen, T. T., Le, H. G., Dao, T.-P., and Huang, S.-C., 2017. “Evaluation of structural behaviour of a novel compliant prosthetic ankle-foot”. In 2017 International Conference on Mechanical, System and Control Engineering (ICMSEC), IEEE, pp. 58–62.
- [16] Zubair, M., and Jung, S., 2022. “Design and analysis of flexure joint for a flexible robotic arm”. In 2022 13th Asian Control Conference (ASCC), IEEE, pp. 2201–2205.
- [17] Vittor, T., Staab, H., Breisch, S., Soetebier, S., Stahl, T., Hackbarth, A., and Kock, S., 2011. “A flexible robotic gripper for automation of assembly tasks: A technology study on a gripper for operation in shared human environments”. In 2011 IEEE International Symposium on Assembly and Manufacturing (ISAM), IEEE, pp. 1–6.
- [18] Goldfarb, M., and Celanovic, N., 1999. “A flexure-based gripper for small-scale manipulation”. *Robotica*, **17**(2), pp. 181–187.
- [19] Li, W., Zhang, D., Yang, G.-Z., and Lo, B., 2022. “Design and modelling of a spring-like continuum joint with variable pitch for endoluminal surgery”. In 2022 IEEE/RSJ International Conference on Intelligent Robots and Systems (IROS), IEEE, pp. 41–47.
- [20] Osawa, K., Bandara, D., Nakadate, R., Nagao, Y., Akahoshi, T., Eto, M., and Arata, J., 2023. “2.5-mm articulated endoluminal forceps using a compliant mechanism”. *International Journal of Computer Assisted Radiology and Surgery*, **18**(1), pp. 1–8.
- [21] Berthet-Rayne, P., Leibrandt, K., Kim, K., Seneci, C. A., Shang, J., and Yang, G.-Z., 2018. “Rolling-joint design optimization for tendon driven snake-like surgical robots”. In 2018 IEEE/RSJ international conference on intelligent robots and systems (IROS), IEEE, pp. 4964–4971.
- [22] Bandara, D., Nakadate, R., Marinho, M. M., Harada, K., Mitsuishi, M., and Arata, J., 2023. “3.5 mm compliant robotic surgical forceps with 4 dof: design and performance evaluation”. *Advanced Robotics*, **37**(4), pp. 270–280.
- [23] Jainandunsing, S., Herder, J. L., Takeda, Y., and Matsuura, D., 2016. “Design of a compliant environmentally interactive snake-like manipulator”. In ROMANSY 21-Robot Design, Dynamics and Control: Proceedings of the 21st CISM-IFTOMM Symposium, June 20–23, Udine, Italy, Springer, pp. 233–240.
- [24] Zhao, H., Zhao, C., Ren, S., and Bi, S., 2019. “Analysis and evaluation of a near-zero stiffness rotational flexural pivot”. *Mechanism and Machine Theory*, **135**, pp. 115–129.
- [25] Morsch, F. M., and Herder, J. L., 2010. “Design of a generic zero stiffness compliant joint”. In International Design Engineering Technical Conferences and Computers and Information in Engineering Conference, Vol. 44106, pp. 427–435.
- [26] Kuppens, P., Bessa, M., Herder, J. L., and Hopkins, J., 2021. “Compliant mechanisms that use static balancing to achieve dramatically different states of stiffness”. *Journal of Mechanisms and Robotics*, **13**(2), p. 021010.
- [27] Kuppens, P., Bessa, M., Herder, J., and Hopkins, J., 2021. “Monolithic binary stiffness building blocks for mechanical digital machines”. *Extreme Mechanics Letters*, **42**, p. 101120.
- [28] Hoetmer, K., Woo, G., Kim, C., and Herder, J., 2010. “Negative stiffness building blocks for statically balanced compliant mechanisms: design and testing”.
- [29] Rijff, B. L., Herder, J. L., and Radaelli, G., 2011. “An energy approach to the design of single degree of freedom gravity balancers with compliant joints”. In International Design Engineering Technical Conferences and Computers and Information in Engineering Conference, Vol. 54839, pp. 137–148.
- [30] Gallego, J. A., 2013. “Statically balanced compliant mechanisms”.
- [31] Merriam, E. G., Colton, M., Magleby, S., and Howell, L. L., 2013. “The design of a fully compliant statically balanced mechanism”. In International Design Engineering Technical Conferences and Computers and Information in Engineering Conference, Vol. 55935, American Society of Mechanical Engineers, p. V06AT07A035.
- [32] Kucuk, S., and Bingul, Z., 2006. *Robot kinematics: Forward and inverse kinematics*. INTECH Open Access Publisher London, UK.
- [33] Howell, L. L., and Midha, A., 1994. “A method for the design of compliant mechanisms with small-length flexural pivots”.
- [34] Howell, L. L., 2013. “Compliant mechanisms”. In 21st Century Kinematics: The 2012 NSF Workshop, Springer, pp. 189–216.
- [35] Yang, Y., Wu, Y., Li, C., Yang, X., and Chen, W., 2020.

- “Flexible actuators for soft robotics”. *Advanced Intelligent Systems*, **2**(1), p. 1900077.
- [36] Lendlein, A., and Kelch, S., 2002. “Shape-memory polymers”. *Angewandte Chemie International Edition*, **41**(12), pp. 2034–2057.
- [37] Majidi, C., 2014. “Soft robotics: a perspective—current trends and prospects for the future”. *Soft robotics*, **1**(1), pp. 5–11.
- [38] Walker, J., Zidek, T., Harbel, C., Yoon, S., Strickland, F. S., Kumar, S., and Shin, M., 2020. “Soft robotics: A review of recent developments of pneumatic soft actuators”. In *Actuators*, Vol. 9, MDPI, p. 3.
- [39] Majidi, C., 2019. “Soft-matter engineering for soft robotics”. *Advanced Materials Technologies*, **4**(2), p. 1800477.
- [40] Sachyani Keneth, E., Kamyshny, A., Totaro, M., Beccai, L., and Magdassi, S., 2021. “3d printing materials for soft robotics”. *Advanced Materials*, **33**(19), p. 2003387.
- [41] Cormack, J., Fotouhi, M., Adams, G., and Pipe, T., 2021. “Comparison of concentrated and distributed compliant elements in a 3d printed gripper”. In *Annual Conference Towards Autonomous Robotic Systems*, Springer, pp. 193–197.
- [42] Farhadi Machekposhti, D., Tolou, N., and Herder, J., 2015. “A review on compliant joints and rigid-body constant velocity universal joints toward the design of compliant homokinetic couplings”. *Journal of Mechanical Design*, **137**(3), p. 032301.
- [43] Huang, W., Ding, Z., Wang, C., Wei, J., Zhao, Y., and Purnawali, H., 2010. “Shape memory materials”. *Materials today*, **13**(7-8), pp. 54–61.

2

Appendices

A Reasoning behind the Project

Flexible robots is a field of robotics that focuses on the development and application of robots with flexible, adaptable, and often soft structures. Unlike traditional rigid robots, flexible robots can bend, stretch, and conform to their environments, which makes them suitable for a wide range of applications that require delicate handling, adaptability, and safe interaction with humans and the environment. There is a need for flexible robotics due to the limitations of rigid robotics, such as the environmental sensitivity, limited flexibility and safety concerns. Rigid robots may struggle in dynamic and unpredictable environments, for example when the robot is required in medical or search and rescue applications. But while all of this sounds promising, there are enough reasons to believe that flexible robotics will not replace the tradition rigid robotics but simply add another dimension to the field [35].

There are two main kinds of flexible robotics are modular continuum robotics and soft robotics of which the latter is the best known. Soft robotics is a subfield that focuses on the use of soft materials to construct the body. The starting point for most soft robotics are bio-inspired [36–39], which means that inspiration for the mechanism has been taken from nature, and the materials used have a large variety from fluids, hydrogels, acrylonitrile butadiene styrene (ABS) and epoxy resins. With the help of a pneumatic, hydraulic or electrostatic actuation methods, these kinds of robots are ideal for grasping fragile objects or locomotion [40]. The second kind of flexible robots focus more on the configurational side of robotics, utilizing compliant mechanisms to make flexible and deformable structures. These fundamentals provide the mechanism with more precision and predictability than soft structures. The movement is often more deterministic, making them suitable for applications requiring high accuracy and repeatability. Together with the rising technology in 3D-printing, there are less material and design complexities. For these reasons, it has been decided to focus this research on these structural kind of mechanism utilizing compliant mechanisms.

Compliant mechanisms do not make use of rigid links and traditional joints, but members that are able to bend along their length [12]. This bending is possible due to the elastic deformation in the chosen material and the configuration in which the members have been designed. This deflection can result in movement with desirable characteristics, such as frictionless motion and minimal particle production. The mechanism requires little to no assembly, needs no lubrication, and is compact, though it can be very complex. However, there are also disadvantages, such as non-linearities from large deflections, limited rotation angles, the need for fatigue analysis, and relative difficulty in design [34]. Compliant mechanisms have two fundamental subdivisions: distributed and concentrated compliant elements. Concentrated compliance has a mostly rigid flexure with a small concentrated region where elastic deformation is possible due to a change in shape and could be used as a straight joint. Distributed compliance has a larger, less concentrated region which distributes the stress concentration and thus results in a larger possible deflection angle and radius [41]. By using these basics, different types of compliant hinges and joints have been designed so that it can be used for various robotic features. These hinges all have different characteristics such as range of motion and on- and off-axis stiffness [42]. In recent years, these types of mechanisms have been developed for various applications, including: Grasping, locomotion, vibration isolators and general manipulators.

Despite advancements in technology, state-of-the-art systems face inherent limitations. High-precision applications often require machines to operate in vacuum environments, while robotic manipulators need increased flexibility for underwater or space tasks. However, current flexible robots utilize non-compliant actuation methods, such as rotational electric motors, cable-driven systems, or manual operation. These techniques can produce particles, generate friction, and require lubrication, whereas compliant mechanisms inherently provide benefits like shock absorption, efficiency, lightweight design, and precision. Therefore, there is a critical need for flexible robots to adopt compliant actuation methods using smart materials to fully realize the advantages of compliant mechanisms.

Smart material actuators are devices that have embodied intelligence, which are internal specification with unique properties to generate a mechanical motion or force while stimulated with the correct, external, triggers like an electric or magnetic field, temperature change, light or pH. They are often referred to as smart because they have the ability to alter their properties in a controllable manner which is also reversible. The most well known smart materials are shape memory materials, electro- and magnetostrictive materials and thermoelectric materials. By applying their respective stimuli, these materials can be used as actuators because of the accompanying movement in the materials. Shape memory materials are characterized by their capability to regain their initial shape after undergoing, what seems like, plastic deformation after the correct external stimuli has been applied [43]. This phenomenon is called the shape memory effect (SME) and is used the most in literature in combination with compliant mechanisms. This is due to the high power density that can be found in the subcategory Shape Memory Alloys (SMAs). The most popular alloy is Nitinol which could recover their shape completely when heated above a certain temperature, which is mostly done by applying an electric current over the material. They can undergo large deformations and still return to their original shape, meaning they could be ideal for the use as actuators in macro robotics. However, a limitation arises with the need for increased current as the actuation load increases, leading to lower energy efficiency. As compliant mechanisms face increased internal resistance with larger deformations due to rising potential energy in their flexures, reducing the added actuation load becomes desirable. One way to achieve this is by designing a statically balanced mechanism, which helps minimize the required actuation load.

B Working Principle of PRBM

Its key concept is modelling a compliant mechanisms using rigid links, revolute joints and torsional springs (Figure 15). These springs represent the stiffness of the flexures, while the revolute joints mimic the rotation points of the flexible members. The compliant joints will thus be modeled as linear torsional springs and the potential energy can be described by

$$U_{spring} = \frac{1}{2}k(\phi(\theta, y) - \phi_0)^2, \quad (22)$$

where k is the torsional stiffness, ϕ_0 is the preload angle that needs to be optimized and ϕ is the angular rotation of each joint that is dependent on the DoF. As the mechanism is focussed on two DoF, the angular rotation is dependent on the y -displacement and the rotation of the end effector θ . Optimization of the torsion stiffness and preloads will lead to the finalized parameters of the whole mechanism.

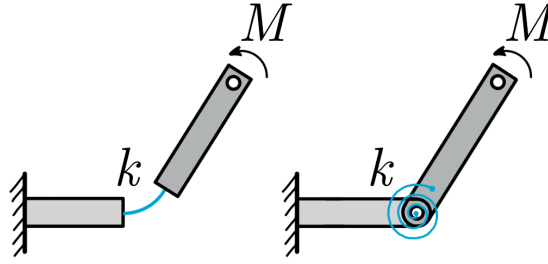


FIGURE 15: Illustration of the working principle of the Pseudo-Rigid Body Model (PRBM), where flexible elements of a compliant mechanism are approximated as rigid links and rotational springs, simplifying the analysis and design of complex compliant systems.

C Explanation of the Implemented Normalization Method and Root-Mean-Square

Normalization of the objective function is a crucial step in optimization, particularly in complex problems involving multiple objectives or different scales of inputs. It ensures that the optimization process is more stable, interpretable, and efficient. It typically results in that the objective values will fall in a certain range between 0 and 1. Normalization can be done in various ways, but for this project it has been decided to look into Min-Max Normalization. This makes it easier to compare and combine different objectives. Min-Max normalization has the form

$$Z_{norm}(\Omega, y_{ij}, \theta_{ij}) = \frac{Z(\Omega, y_{ij}, \theta_{ij}) - f_{min}}{f_{max} - f_{min}} \quad (23)$$

where $Z = (F, M)$ which is either the Force or Moment equation, f_{min} is the lowest possible value and f_{max} is the largest possible value for their respective, non-optimized objective function. By doing so, the functions are dimensionless and reside between 0 and 1 for an accurate comparison in the optimization algorithm.

As the normalized function needs to be reduced to zero over the whole domain, the RMS has been taken of the functions over the entire range. The RMS represents the magnitude of a varying quantity and for this situation it means that it creates a general equation that pulls the objective function for each coordinate to zero. For a set of $n \times n$ datapoints, the RMS is given by:

$$f_{(F,M)} = \sqrt{\frac{1}{n^2} \sum_{i=1}^n \sum_{j=1}^n f_{ij}^2}, \quad (24)$$

where $f_{ij} = Z_{norm}(\Omega, y_{ij}, \theta_{ij})$ and $n = 100$. The value of n can be changed accordingly. Equation 24 essentially means that the equation will be evaluated at every combination of y and θ and makes sure it can be used in the optimisation objective.

D Moment Reduction Plots - Case Study and Compensated Beams

The reduction in moment for both optimized mechanism can be seen in the surf plots. In blue, the unloaded mechanism with the same joint stiffnesses can be seen while the green surf curve shows the preloaded mechanism. The reduction can be calculated by picking out the highest moment values for one specific location and compare them to each other. For $y = 150[mm]$, the reduction is around 50% while for the lowest y -value the reduction is 80%. The reduction for the compensated beams mechanism is more uniform over the whole range, at an approximate reduction of around 95%.

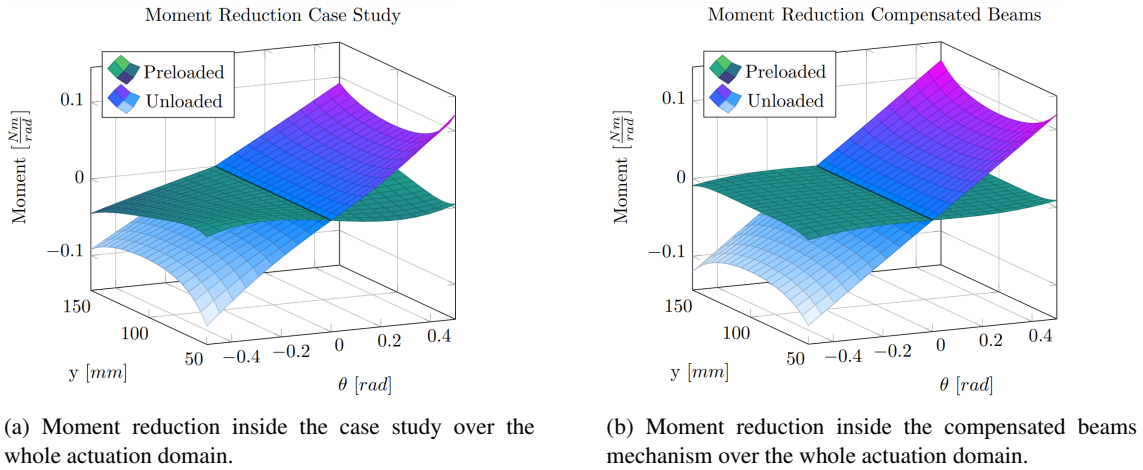
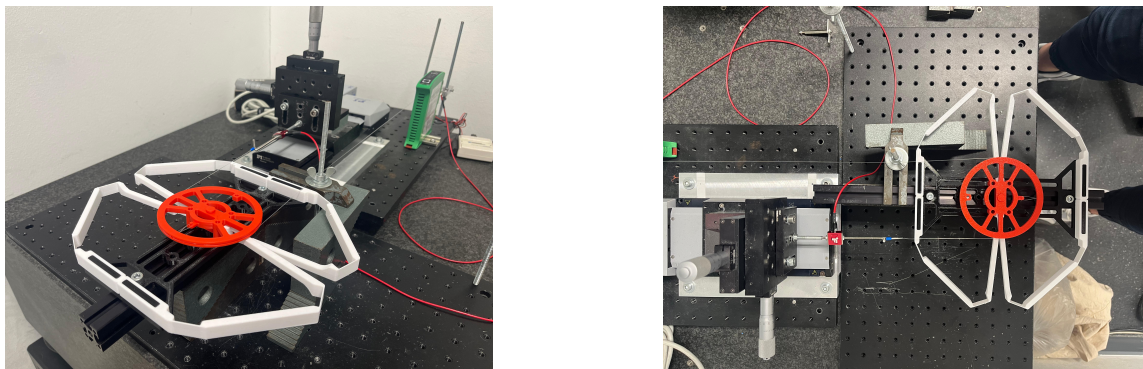


FIGURE 16: Moment plots for both the case study and the compensated beams mechanism.

E Pictures of the Test Setup for Moment Measurements

This test setup removes the direct rigid connection of the sensor to the end effector. To measure a moment, the force normal to the circumference of the end effector has to be measured. This is done by routing a fishing wire around the end effector. Because the neutral position is at $\theta = 0 [rad]$ and fishing wire can only be placed under tension, a counterweight is added at the other end of the end effector. This creates tension on both sides, making sure the sensor essentially measures the internal moment and the counterweight. Now the end effector can be rotated and measured towards both sides.



(a) Side view of the test setup for the moment measurements. The pulley system is located behind the processor (green).

(b) Top view of the test setup. Here you can clearly see the fishing wire running around the end effector (red).

FIGURE 17: Test setup for the moment-rotation measurements from multiple angles.

F First Iterations of the Mechanism

This project started by exploring the fourbar mechanisms found in literature. By replicating the existing papers, a general feeling for preloading compliant mechanisms was found. This knowledge was expanded to a fivebar mechanism, which has 2 DoF. The flexure between link 2 and 3 was the point of interest and the mechanism was optimized to be statically balanced. The reduction was not satisfactory, but a prototype of the mechanism was made using TPU flexures. This first prototype can be seen in Figure 18, where both the manufacturing position and the preloaded mechanism are shown in Figure 18a and 18b respectively. As can be concluded from this iteration, the point of interest does not remain on the centerline of the mechanism but rather more towards the right side. This outcome is expected due to the unconstrained nature of 2-DoF compliant mechanisms. However, it presents a challenge because the actuation methods must counteract this unintended movement, which not only reduces energy efficiency but also complicates the control system. To address these issues, a second iteration was developed.



(a) Design and manufacturing position of the first iteration.



(b) The first iteration with the preload in place.

FIGURE 18: Pictures of the first prototype made for this project. A fivebar was made using TPU flexures and an optimized preload, however the resting position of the mechanism was not symmetrical as can be seen in the right picture.

The idea of the second iteration was to see if symmetrical preloading the joints over the centerline would result in the desired outcome. There were two things to test: 1) Does this keep the point of interest at the desired position and 2) Is a reduction possible while constraining the mechanism to symmetrical stiffness and preloading values. This second iteration can be found in Figure 19. It can be concluded that 1) the point of interest does indeed remain at the intended location. There is no drift of the points of the central line. Additionally, 2) there was still a similar reduction possible while using this symmetric preloading. This meant that the third DoF for a sixbar configuration could be eliminated by preloading the mechanism symmetrically, reducing the complexity of the problem that has to be solved.



(a) Manufacturing position of the second iteration.



(b) Preloaded position of the second iteration.

FIGURE 19: Pictures of the second prototype that has been made to test the hypothesis of symmetrically preloading the mechanism. From the right picture it can be concluded that this indeed works as expected.

G First Prototype of the Compensated Beams Mechanism

The compensated beams mechanism underwent multiple iterations of prototyping, with the first version shown in the bottom left (Figure 20a). This initial prototype was printed to evaluate the shape and feel of the design. Although no preload was applied, the range of motion of the end effector was tested for potential clashes, mobility, and overall feasibility. This early prototype provided valuable insights into how the final product would look and function.

Subsequently, the design was expanded to include the entire mechanism. It was mirrored along the y-axis, and various printing configurations were explored. Due to differences in flexure height, supports were needed during printing, which led to manufacturing errors. As a result, the end effector had an undesired resting position of $\theta = -0.5$ [rad]. Further testing involved designing the flexures near the end effector either stacked on top of each other or side by side. Both configurations were functional, but the stacked design resulted in fewer clashes.

After these iterations, the final printing method was selected. This involved printing each arm separately, with the height differences between the flexures ensuring that the arms did not interfere with each other. Rapid prototyping of multiple configurations played a crucial role in refining the design and arriving at a solution that worked for all requirements.

H Material Selection of the Flexures

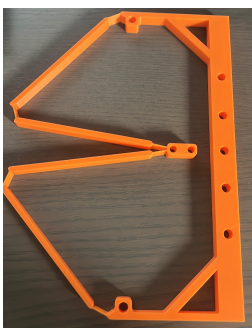
The material selection for the flexures was not solely based on calculations from the equations in the referenced paper, but also through physical testing. This approach was taken to gain a hands-on understanding of the rotation limit defined by Howell et al. and to address uncertainties that arose from the calculation results.

These uncertainties stemmed from the fact that calculations suggested steel flexures would need to be 50[mm] long and extremely thin to achieve a total bend of 1.344[rad] without experiencing plastic deformation. While the calculations were technically correct, intuition suggested that a shorter length might still be feasible. To test this, a setup was designed and printed (Figure 20b) that allowed for testing flexures of varying lengths and thicknesses up to the rotation limit. The test included steel flexures, as well as those made from PLA, PETG, and TPU. From these experiments, it was confirmed that the steel flexure did indeed undergo plastic deformation under the specified displacement, while the PETG flexure behaved elastically as predicted by the calculations. This physical testing provided critical confirmation of the material behavior in practice.

I Difference between Unloaded and Preloaded Flexures

The final outcome of all the preceding tests and prototypes is illustrated in Figure 20c. In this design, each arm of the end effector is printed individually without the use of supports, to avoid potential issues introduced by support structures during printing. This method was applied consistently for both the unloaded and preloaded arms, with the key distinction being the angles at which the links were manufactured. The figure clearly shows the precise differences between the unloaded mechanism and the preloaded arms, which contribute to achieving static balancing.

While the difference between the two configurations might appear small at first glance, it has a significant impact on the mechanism's performance. When preloaded, the mechanism operates in the nonlinear region, meaning its behavior becomes more complex due to increased flexure deformation. In this state, the mechanism approaches its physical limits, with the rotation range and yield strength being pushed to the maximum. This fine-tuning of the preloaded mechanism done in the project was essential for optimizing its performance and ensuring reliable operation without compromising structural integrity.



(a) First iteration



(b) Material test bench



(c) Difference between unloaded and preloaded

FIGURE 20: Overview of the numerous steps that had to be taken to get to the end result

J Compensated Beams Matlab Script

```
1 % Initialization
2 clf, hold off, clear
3
4 % Set up the boundary values for all the optimization parameters
5 theta_min = [0.02  0.02  0.02  0.866  0.716  2.906  0.3  -0.1   0];
6 theta_max = [0.1  0.1  0.1      3.224  1.864  3.194   1   0   0.05];
7
8 % Define options for gamultiobj
9 options = optimoptions('gamultiobj', 'PopulationSize', 200, 'MaxGenerations', 500, ...
10     'FunctionTolerance', 1e-6, 'CrossoverFraction', 0.8, 'ParetoFraction', 0.7, ...
11     'MaxStallGenerations', 50, 'PlotFcn', @customGaplotpareto);
12
13 % Run gamultiobj
14 [opt, fval] = gamultiobj(@(x)fivebar_sixbar(x), 9, [], [], [], [], theta_min, theta_max, [], options);
15
16
17 function state = customGaplotpareto(options, state, flag)
18     % Call the original gaplotpareto function to plot the Pareto front
19     gaplotpareto(options, state, flag);
20
21     % Customize the plot
22     ax = gca; % Get current axes handle
23     ax.Color = [1, 1, 1]; % Set background color
24     fig = gcf; % Get current figure handle
25     fig.Color = [1, 1, 1]; % Set figure background color to white
26     ax.XLabel.String = 'Objective 1 (Force)'; % Set x-axis label
27     ax.YLabel.String = 'Objective 2 (Moment)'; % Set y-axis label
28     title('Pareto Front Plot'); % Set title
29 end
```

```
1 %%% Create the function which models the linkage system %%%
2 function f = fivebar_sixbar(x)
3
4 % Setting up the optimization variables
5 k1a = x(1);
6 k2a = x(2);
7 k3a = x(3);
8 phi1a0 = x(4);
9 phi2a0 = x(5);
10 phi3a0 = x(6);
11 delta1 = x(7); %Will be 0.35 after third iteration
12 xa = x(8); %Will be 0.07 after second iteration
13 ya = x(9); %Will be 0 after second iteration
14
15 % After the first iteration, symmetry has been determined over the x-axis
16 k1b = k1a;
17 k2b = k2a;
18 k3b = k3a;
19 phi1b0 = phi1a0;
20 phi2b0 = phi2a0;
21 phi3b0 = phi3a0;
22 delta2 = delta1;
23 xb = xa;
24 yb = ya;
25
26 % Describe the maximum values of the actuation range
27 y_min = 0.05;
28 y_max = 0.15;
29 theta_min = -0.5;
30 theta_max = 0.5;
31
32 % Set up the ranges
```

```

33 h = 0.001;           % Central differential approximation step size
34 y = y_min:h:y_max;
35 theta = theta_min:h:theta_max;
36 [Y, THETA] = meshgrid(y, theta);   % Create 2D grid
37
38 % Set up linkage parameters
39 L1 = 0.1;
40 L2 = L1;
41 L_EE = L1;
42 x = 0;           %x has been set to zero
43
44 %%% Make descriptions for all the rotations happening in the mechanism %%%
45 % Bottom left linkage modelling
46 xcb = x - delta1 * L_EE * cos(THETA);
47 ycb = Y - delta1 * L_EE * sin(THETA);
48
49 Ra = sqrt((ycb - ya).^2 + (xcb - xa).^2);
50 phi1a = acos((L1.^2 + Ra.^2 - L2.^2) ./ (2 * L1 * Ra)) + atan2((ycb - ya), (xcb - xa));
51 phi2a = acos((L1.^2 + L2.^2 - Ra.^2) ./ (2 * L1 * L2));
52 phi3a = acos((L2.^2 + Ra.^2 - L1.^2) ./ (2 * L2 * Ra)) + atan2((xcb - xa), (ycb - ya)) + 0.5 * pi + THETA;
53
54 % Top left linkage modelling
55 xct = x - delta2 * L_EE * cos(THETA);
56 yct = (0.2 - Y) + delta2 * L_EE * sin(THETA);
57
58 Rb = sqrt((yct - yb).^2 + (xct - xb).^2);
59 phi1b = acos((L1.^2 + Rb.^2 - L2.^2) ./ (2 * L1 * Rb)) + atan2((yct - yb), (xct - xb));
60 phi2b = acos((L1.^2 + L2.^2 - Rb.^2) ./ (2 * L1 * L2));
61 phi3b = acos((L2.^2 + Rb.^2 - L1.^2) ./ (2 * L2 * Rb)) + atan2((xct - xb), (yct - yb)) + 0.5 * pi - THETA;
62
63 % Bottom right linkage modelling
64 x3 = x - delta1 * L_EE * cos(THETA);
65 y3 = Y + delta1 * L_EE * sin(THETA);
66
67 Rc = sqrt((y3 - ya).^2 + (x3 - xa).^2);
68 phi1c = acos((L1.^2 + Rc.^2 - L2.^2) ./ (2 * L1 * Rc)) + atan2((y3 - ya), (x3 - xa));
69 phi2c = acos((L1.^2 + L2.^2 - Rc.^2) ./ (2 * L1 * L2));
70 phi3c = acos((L2.^2 + Rc.^2 - L1.^2) ./ (2 * L2 * Rc)) + atan2((x3 - xa), (y3 - ya)) + 0.5 * pi - THETA;
71
72 % Top right linkage modelling
73 x4 = x - delta2 * L_EE * cos(THETA);
74 y4 = (0.2 - Y) - delta2 * L_EE * sin(THETA);
75
76 Rd = sqrt((y4 - yb).^2 + (x4 - xb).^2);
77 phi1d = acos((L1.^2 + Rd.^2 - L2.^2) ./ (2 * L1 * Rd)) + atan2((y4 - yb), (x4 - xb));
78 phi2d = acos((L1.^2 + L2.^2 - Rd.^2) ./ (2 * L1 * L2));
79 phi3d = acos((L2.^2 + Rd.^2 - L1.^2) ./ (2 * L2 * Rd)) + atan2((x4 - xb), (y4 - yb)) + 0.5 * pi + THETA;
80
81 % Potential energy equations consisting of stiffness values, preloads and rotations
82 U1a = 0.5 * k1a * (phi1a - phi1a0).^2;
83 U2a = 0.5 * k2a * (phi2a - phi2a0).^2;
84 U3a = 0.5 * k3a * (phi3a - phi3a0).^2;
85 U1b = 0.5 * k1b * (phi1b - phi1b0).^2;
86 U2b = 0.5 * k2b * (phi2b - phi2b0).^2;
87 U3b = 0.5 * k3b * (phi3b - phi3b0).^2;
88 U1c = 0.5 * k1a * (phi1c - phi1a0).^2;
89 U2c = 0.5 * k2a * (phi2c - phi2a0).^2;
90 U3c = 0.5 * k3a * (phi3c - phi3a0).^2;
91 U1d = 0.5 * k1b * (phi1d - phi1b0).^2;
92 U2d = 0.5 * k2b * (phi2d - phi2b0).^2;
93 U3d = 0.5 * k3b * (phi3d - phi3b0).^2;
94
95 % Total potential energy equation of the system
96 U_tot = @(Y, THETA) U1a + U2a + U3a + U1b + U2b + U3b + U1c + U2c + U3c + U1d + U2d + U3d;

```

```

97
98 % Setting up the central differential approximation equations
99 objective = U_tot(Y, THETA);
100 [n1, n2] = size(Y);
101 dy = zeros(n1, n2);
102 dphi = zeros(n1, n2);
103
104 % Take the central differential approximation for both the moment and the force derivative
105 for i = 2:n1-1
106     for j = 2:n2-1
107         dphi(i, j) = (objective(i+1, j) - objective(i-1, j)) / (2 * h);
108         dy(i, j) = (objective(i, j+1) - objective(i, j-1)) / (2 * h);
109     end
110 end
111
112 % Normalize the equations and take the RMS over the whole system
113 force = rms(dy/2.6, 'all');           %Maximum force is 2.6N, minimum is 0N.
114 moment = rms(dphi/0.13, 'all');      %Maximum moment is 0.13Nm/rad, minimum is 0Nm/rad
115
116 % Create the final two equations that can be used as objective functions
117 f = [force moment];
118 end

```

K Ansys Code for Force-Displacement on Preloaded Mechanism

```
1  !!! Clear program
2  FINISH
3  /CLEAR
4  /OUTPUT
5
6
7  ! Define values parameters
8  n = 50
9  s = 100
10
11 L_EE = 35e-3
12 L_flexure = 20e-3
13 L_member = 100e-3
14 L_base = 70e-3
15
16 PI = 3.141592653589793
17
18 preload1 = 0.91
19 preload2 = 1.82
20 preload3 = 3.01
21
22 ! Calculate all the positions of the keypoints
23 n1x = 0
24 n1y = 0
25 n2x = n1x + cos(0)*L_EE - 0.5*L_flexure
26 n2y = n1y
27 n3x = n2x + cos(0)*L_flexure
28 n3y = n1y
29
30 x_f12 = n3x - 0.5*L_flexure + L_member*cos(pi-preload3)
31 y_f12 = n3y + L_member*sin(pi-preload3)
32
33 n4x = x_f12 - cos(0.5*pi-0.5*preload2 + pi - preload3)*0.5*L_flexure
34 n4y = y_f12 - sin(0.5*pi-0.5*preload2 + pi - preload3)*0.5*L_flexure
35 n5x = x_f12 + cos(0.5*pi-0.5*preload2 + pi - preload3)*0.5*L_flexure
36 n5y = y_f12 + sin(0.5*pi-0.5*preload2 + pi - preload3)*0.5*L_flexure
37
38 x_f11 = x_f12 - cos(preload2-(pi-preload3))*L_member
39 y_f11 = y_f12 + sin(preload2-(pi-preload3))*L_member
40
41 n6x = x_f11 + cos(preload2-(pi-preload3)-(0.5*pi-0.5*preload1))*0.5*L_flexure
42 n6y = y_f11 - sin(preload2-(pi-preload3)-(0.5*pi-0.5*preload1))*0.5*L_flexure
43 n7x = x_f11 - cos(preload2-(pi-preload3)-(0.5*pi-0.5*preload1))*0.5*L_flexure
44 n7y = y_f11 + sin(preload2-(pi-preload3)-(0.5*pi-0.5*preload1))*0.5*L_flexure
45 n8x = n7x - cos(pi-(preload2-(pi-preload3)+preload1))*(L_base-sin(0.523598776))*0.5*L_flexure)
46 n8y = n7y - sin(pi-(preload2-(pi-preload3)+preload1))*(L_base-sin(0.523598776))*0.5*L_flexure)
47
48 L_base = sqrt((n8x-n7x)**2 + (n8y-n7y)**2)
49
50 n8x_disp = (0-n8x)
51 n8y_disp = (0.10+cos(30*(pi/180))*0.5*L_flexure)-n8y
52 n7x_disp = 0+L_base-n7x
53 n7y_disp = (0.10+cos(30*(pi/180))*0.5*L_flexure)-n7y
54
55 ! Define preload displacements
56 my = 25e-3*sin(0.5)
57 mx = (25e-3 - 25e-3*cos(0.5))
58
59
60 !!! Enter pre-processor
61 /prep7
62
```

```

63 ! Define element type
64 et,1,BEAM188
65 et,2,MPC184,1
66 KEYOPT,2,1,1
67
68 ! Define cross section
69 /ESHAPE,1
70 sectype,1,beam,rect,flexure_small
71 secdata, 0.8e-3, 4.8e-3
72
73
74 /ESHAPE,1
75 sectype,2,beam,rect,flexure_medium
76 secdata, 0.8e-3, 12.6e-3
77
78 /ESHAPE,1
79 sectype,3,beam,rect,flexure_big
80 secdata, 0.8e-3,13e-3
81
82 ! Define material properties
83 mp,ex,1,2e9
84 mp,prxy,1,0.33
85
86 ! Make keypoints
87 k,1,n1x,n1y,0
88 k,2,n2x,n2y,0
89 k,3,n3x,n3y,0
90 k,4,n4x,n4y,0
91 k,5,n5x,n5y,0
92 k,6,n6x,n6y,0
93 k,7,n7x,n7y,0
94 k,8,n8x,n8y,0
95 k,9,n3x,-n3y,0
96 k,10,n4x,-n4y,0
97 k,11,n5x,-n5y,0
98 k,12,n6x,-n6y,0
99 k,13,n7x,-n7y,0
100 k,14,n8x,-n8y,0
101 k,15,-n2x,n2y,0
102 k,16,-n3x,n3y,0
103 k,17,-n4x,n4y,0
104 k,18,-n5x,n5y,0
105 k,19,-n6x,n6y,0
106 k,20,-n7x,n7y,0
107 k,21,-n8x,n8y,0
108 k,22,-n3x,-n3y,0
109 k,23,-n4x,-n4y,0
110 k,24,-n5x,-n5y,0
111 k,25,-n6x,-n6y,0
112 k,26,-n7x,-n7y,0
113 k,27,-n8x,-n8y,0
114
115 ! Define lines and respective material properties
116 *GET, ID1, LINE, , NUM, MAXD
117 L,2,3
118 L,2,9
119 L,15,16
120 L,15,22
121
122 *GET, ID2, LINE, , NUM, MAXD
123 L,4,5
124 L,10,11
125 L,17,18
126 L,23,24

```

```

127
128 *GET, ID3, LINE, , NUM, MAXD
129 L, 6, 7
130 L, 12, 13
131 L, 19, 20
132 L, 25, 26
133
134 *GET, ID4, LINE, 0, NUM, MAXD
135 L, 1, 2
136 L, 3, 4
137 L, 5, 6
138 L, 7, 8
139 L, 9, 10
140 L, 11, 12
141 L, 13, 14
142
143 L, 1, 15
144 L, 16, 17
145 L, 18, 19
146 L, 20, 21
147 L, 22, 23
148 L, 24, 25
149 L, 26, 27
150 *GET, ID5, LINE, 0, NUM, MAXD
151 ! Mesh all the lines
152 type, 1
153 mat, 1
154 secnum, 1
155 lsel, s, line, , ID1+1, ID2
156 lesize, all, , , n
157 lmesh, all
158
159 allsel, all
160
161 type, 1
162 mat, 1
163 secnum, 2
164 lsel, s, line, , ID2+1, ID3
165 lesize, all, , , n
166 lmesh, all
167
168 allsel, all
169
170 type, 1
171 mat, 1
172 secnum, 3
173 lsel, s, line, , ID3+1, ID4
174 lesize, all, , , n
175 lmesh, all
176
177 ALLSEL, ALL
178
179 TYPE, 2
180 LSEL, S, LINE, , ID4+1, ID5
181 LESIZE, ALL, , , 1
182 LMESH, ALL
183
184 ! Apply boundary conditions
185 dk, 1, all, 0
186
187 ! Apply preload displacements on all flexures
188 dk, 7, uy, n7y_disp
189 dk, 8, ux, n8x_disp
190 dk, 8, uy, n8y_disp

```

```

191
192 dk,13,uy,-n7y_disp
193 dk,14,ux,n8x_disp
194 dk,14,uy,-n8y_disp
195
196 dk,20,uy,n7y_disp
197 dk,21,ux,-n8x_disp
198 dk,21,uy,n8y_disp
199
200 dk,26,uy,-n7y_disp
201 dk,27,ux,-n8x_disp
202 dk,27,uy,-n8y_disp
203 finish
204
205
206 !!! Enter the solution processor
207 /solu
208 antype, static
209 nlgeom, on
210 eqslv, sparse
211 outres, all, all
212 autots, on
213 neqit, 100
214 nsubst,1000,,10
215
216 ! Step 1: Move keypoints 7 and 8
217 time,1
218 solve
219
220 ! Step 2: Move end effector to y = +50mm position
221 time,2
222 dk,1,uy,50e-3
223 solve
224 finish
225
226
227
228 ! Enter post-processor
229 /post1
230 set,2,last
231 pldisp,1
232
233 ! Select keypoint 1 on which the force is measured
234 KSEL,S,,1
235 NSLK,S
236 *GET, K1,NODE,0,NUM,MIN
237 ALLSEL,ALL
238 FINISH
239
240 !!! Enter data extraction processor
241 /POST26
242 NUMVAR,200
243
244 ! Store displacement and force on keypoint 1
245 NSOL,2,K1,U,Y, DY
246 STORE,MERGE
247 RFORCE,3,K1,F,Y, FY
248 STORE,MERGE
249
250 ! Plot force-displacement graph
251 /POST26
252 XVAR,2
253 PLVAR,3

```

L Ansys Code for Moment-Rotation on Preloaded Mechanism

```
1  !!! All the code is the same as in Appendix B, however the steps taken in the solution
2  !!! processor are different:
3
4  ! Step 1: Move keypoints 7 and 8
5  time,1
6  solve
7
8  ! Step 2: Apply a rotation on keypoint 1 of 0.5[rad]
9  time,2
10 dk,1,rotz,0.5
11 solve
12
13 ! Step 3: Rotate keypoint 1 back to original position
14 time,3
15 dk,1,rotz,0
16 solve
17 finish
18
19 !!! Enter post-processor
20 /post1
21 set,2,last
22 pldisp,1
23
24 ! Select keypoint 1
25 KSEL,S,,,1
26 NSLK,S
27 *GET, K1,NODE,0,NUM,MIN
28 ALLSEL,ALL
29 FINISH
30
31 !!! Enter data extraction processor
32 /POST26
33 NUMVAR,200
34
35 ! Store rotation and moment
36 NSOL,2,K1,ROT,Z, DZ
37 STORE,MERGE
38 RFORCE,3,K1,M,Z, MZ
39 STORE,MERGE
40
41 ! Plot moment-rotation graph
42 /POST26
43 XVAR,2
44 PLVAR,3
```

M Ansys Code for Unloaded Mechanism

```
1 !!! All the code is the same for the force and moment simulations, except:
2
3 ! Update the preload angles to the unloaded angles
4 preload1 = 2.25
5 preload2 = 1.12
6 preload3 = 2.92
7
8 ! Replace preload displacements of all keypoints with boundary conditions
9 dk,1,all,0
10 dk,7,all,0
11 dk,8,all,0
12 dk,13,all,0
13 dk,14,all,0
14 dk,20,all,0
15 dk,21,all,0
16 dk,26,all,0
17 dk,27,all,0
```

3

Literature Review

DELFT UNIVERSITY OF TECHNOLOGY

ME-HTE LITERATURE RESEARCH

ME51010-20

A Review of Compliant Mechanisms and Smart Material Actuators for Flexible Robotics

Author:

T.Q. Vis (4699173)

Supervisor:
Daily Supervisor

Prof.Dr.Ir. J.L. Herder
Dr. J. Jovanova

Department of Precision and Microsystems Engineering
Faculty of Mechanical, Maritime and Materials Engineering
Delft University of Technology
Delft, The Netherlands
March 14, 2024



Abstract: In the face of increasingly unpredictable industrial environments, traditional rigid robots encounter limitations, prompting exploration into flexible robotics as a promising solution. Flexible robotics, equipped with shape-changing mechanisms and compliance, offer potential breakthroughs, yet challenges persist in refining actuation methods and exploring new mechanisms beyond soft robots. This literature study aims to provide a comprehensive overview of compliant mechanisms and smart material actuators for use in flexible robotics while pinpointing existing gaps in the literature. While soft robots that use pneumatic actuation methods are widely discussed, they lie outside of the scope because a substantial body of literature already exists on this topic. Employing a systematic review protocol, the study delves into the utilization of compliant mechanisms in flexible robotics, followed by an exploration of smart material actuators on compliant structures. While compliance is integral to flexible robotics, particularly in body or end effectors, actuation mechanisms often lack compliance, relying on cables, electric motors, or manual operation. Smart material actuators emerge as a potential compliant actuation method, yet literature reveals limited exploration beyond fundamental testing, with a notable absence of structural mechanisms for real-life applications. Identifying this gap, the study underscores the need for mechanisms bridging fundamental practices and practical implementation, presenting an opportunity for enhancing future robotic endeavors.

Keywords: Flexible Robotics, Smart Materials, Compliant Mechanisms, Actuation

I. INTRODUCTION

In today's world, a robot is a device that can perform tasks autonomous (or semi-autonomous) and are designed to carry out a variety of actions through physical interaction with the environment [1]. Robots can range from simple devices programmed for specific tasks to highly complex systems equipped with advanced sensors and artificial intelligence, enabling them to adapt to changing conditions. The need for robotics originated from the need of human necessities and led to the start of the use of robots in the industrial world [2]. Robots were applied to the areas of the factory that were risky and harmful for humans, for example manufacturing jobs and car assemblies. Known as the first generation of industrial robots [3], these robots were very difficult to control and could only handle simple tasks of loading and unloading of parts. Ten years later and the robots would evolve into more mature mechanisms due to the use of servo controllers that could perform more difficult tasks, but were still programmed to fulfill only one specific task. The extent of flexibility was constrained. At the end of the 20th century, the robots were far more sophisticated due to updated control systems and learning algorithms so robots can change their operation conditions

for a diversity of tasks. Applications for these kinds of robotics are the medical field for surgery and other human social needs or assembly robotics. But it is for certain that these robots, and the evolution of them, have changed the industry in terms of efficiency, safety, removing maddening repetitive tasks and also advancements in healthcare.

The need for automation of non repetitive tasks and environments leads to the need of flexible robotics. This field refers to the design and development of robotics systems that have the ability to adapt and adjust their movement, structure or function according to a specific environment or task. These robots can do this to navigate challenging environments, handle fragile objects or perform a multiple of tasks. They are more versatile, are cost and space efficient and allow for rapid prototyping and better collaboration with humans. While all of this sounds promising, there are enough reasons to believe that flexible robotics will not replace the traditional rigid robotics but simply add another dimension to the field [4]. There is a need for flexible robotics due to the limitations of rigid robotics, such as the environmental sensitivity, limited flexibility and safety concerns. Rigid robots may struggle in dynamic and unpredictable environments, for example when the robot is required to make shape changes that have not been accounted for during programming. Together with this, rigid robots are designed for fixed structures which means that they struggle to adapt to environments that require flexibility like tight spaces.

There are two main kinds of flexible robotics: modular continuum robotics and soft robotics, of which the latter is the best known. Soft robotics is a subfield that focuses on the use of soft materials to construct the body. The starting point for most soft robotics are bio-inspired [5, 6, 7, 8], which means that inspiration for the mechanism has been taken from nature, and the materials used have a large variety from fluids, hydrogels, acrylonitrile butadiene styrene (ABS) and epoxy resins. With the help of a pneumatic, hydraulic or electrostatic actuation methods, these kinds of robots are ideal for grasping fragile objects or locomotion [9]. This technique is being used, for example, in the soft locomotion of a fish, gripper applications, octopus inspired robotics, human interaction [10], inflatable robotic arms and artificial muscles [11, 7, 12, 13, 14]. But because these soft robotics have a low carrying capacity and are quite limited, for this review, there will be no further investigation in the use of soft robots in the search for the next step in flexible robotics.

The second part of flexible robotics is more focused on the adaptability of their movement or structure, of which the body consists of flexible and deformable structures or in other words compliant mechanisms. This body is coupled with an actuation method to create the desired motion and structure. Compliant mechanisms make use of flexible members to create the desired motion while creating benefits such as no particle production and no lubrication needed. Continuum robots are well known examples of

such flexible robotics, although the actuation methods are largely not compliant which defeats the purpose of the advantages. And while compliant actuation methods exist, they are often not implemented in the whole application. This leads to gaps that could be explored to find out what the next big thing could be for flexible robotics.

The aim of this paper is to provide an overview of the recent advances within the field of flexible robotics. This will be done by finding the state-of-the-art literature on the use of compliant mechanisms for flexible robots and the potential benefit of smart material actuators and by evaluating the results of these areas to make recommendations for future research steps for the development of the next sophisticated flexible robots. To create the best possible overview, the following questions will be answered: What are the relevant compliant mechanisms used in flexible robotics and what are the challenges that present themselves? What types of smart material actuators could be of value for the next generation flexible robotics? And what could potentially be a way forward?

The paper starts with [section II](#) that gives the search methodology used in this paper to get a better understanding of the specific strict search that has been performed. In [section III](#) the literature review starts by investigating the different compliant mechanisms used in the state-of-the-art literature for flexible robotics to get a feeling for the challenges that are present. Based on these challenges, a research gap is found that is discussed in [section IV](#) where all the recent technologies are highlighted. In [section V](#) the previous sections will be evaluated to propose a way forward for the development of flexible robotics for the future.

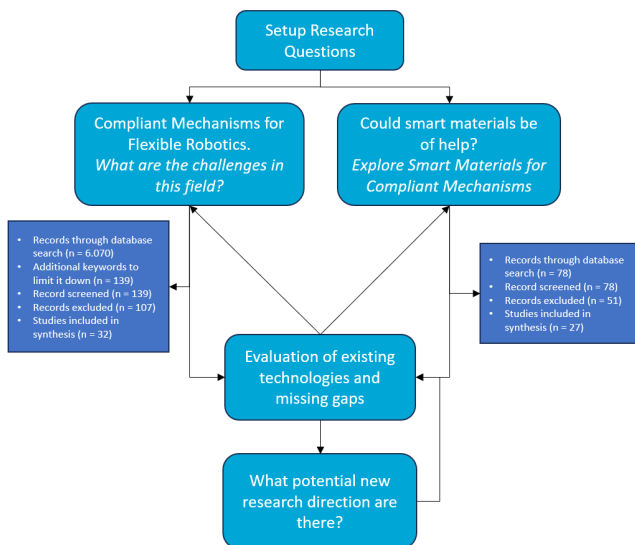


Fig. 1: Flowchart for the literature search and the paper

II. SEARCH METHODOLOGY

Following the research question set up for this paper, it was essential for the literature search to come up with the correct research structure. In [Figure 1](#), the flowchart for the literature search and this paper is visualised. From the research questions, the first step is to investigate the current state-of-the-art for compliant mechanisms in the field of flexible robotics during which the challenges for the next big thing can be identified. Using this knowledge, a proposition has been made that could be of value to the evolving technologies. The options are explored and in the end of the paper a conclusion with recommendations for future work has been made.

The approach used in this literature review has a clearly defined search strategy and has strict inclusion and exclusion criteria. The strict search for this paper is on compliant mechanisms for flexible robotics and this gave the following search terms and results for the first section of the paper. "Compliant Mechanism*" and Flexible and Robot* gives 6.070 results which is too broad to make conclusions on this specific topic. Adding the words together to create "Flexible Robot*" as a search term results in 139 results. Based on relevance, 32 papers have been selected that are of value for the review. This limitation could be made because the majority of the papers would discuss the possible control systems behind the compliance of certain mechanisms or robots, while the scope for this paper lies on the compliant mechanisms themselves, and a few other papers that were ruled out demonstrated the use of soft robotics.

For the second part of this paper, the scope was strictly limited to state-of-the-art literature of the use of smart material actuators for compliant mechanisms. This left the scope with the following keywords and results. "Smart Material Actuator/Actuation" and "Compliant Mechanism*" give a combined result of 78 papers of which 27 have been selected by the same selection method as the last section. The papers that were ruled out were focused on control systems and optimization or modelling techniques for theoretical practices rather than the smart material mechanisms themselves, which is out of scope and therefore not considered in this paper.

III. COMPLIANT MECHANISMS FOR FLEXIBLE ROBOTICS

Unlike traditional robots, flexible robots have bodies that have the ability to bend, stretch or deform in order to adapt to multiple tasks and environments. This field encompasses various sub-disciplines and technologies which can be split up in soft robotics, compliant mechanisms and continuum robots.

Compliant mechanisms and continuum robots are closely related because continuum robots do not have rigid links and traditional joints in their body, but structures that are able to bend along their length [15]. This bending

is possible due to the elastic deformation in the chosen material and the configuration in the design of the mechanisms, known as a compliant mechanism. Compliant mechanisms have the ability to move due to the deflection in flexible members and by using this technique it creates a number of advantages. Compliant mechanisms require little to no assembly, move without friction and thus particle production, need no lubrication, are compact but can be very complex. They also have some disadvantages like nonlinearities, limited rotation angles, they are relatively difficult to design and need fatigue analysis [16]. The basis of compliant mechanisms consists of 2 general subdivisions: distributed and concentrated compliant elements. Concentrated, or lumped, compliance is where the flexure is mostly rigid, but has a small concentrated region where elastic deformation is possible to create a hinge as seen in Figure 2a. Concentrated compliant joints can be put in multiple configurations to create the mechanisms with the desired output and movement. In Figure 2c it can be seen how putting concentrated joints in series can contribute to a compliant four bar mechanism. Distributed compliance is where the region is spread over a much larger area which distributes the stress concentration and gives a large deflection angle and radius [17], which can be seen in Figure 2b. The different types of flexure can be straight or pre-shaped as seen in Figure 2d to create different stiffness characteristics on the end effector visualised in light blue. These flexures can also be combined in a cross leaf flexure like the one in Figure 3a to create a lower stiffness and bigger deflection angle.

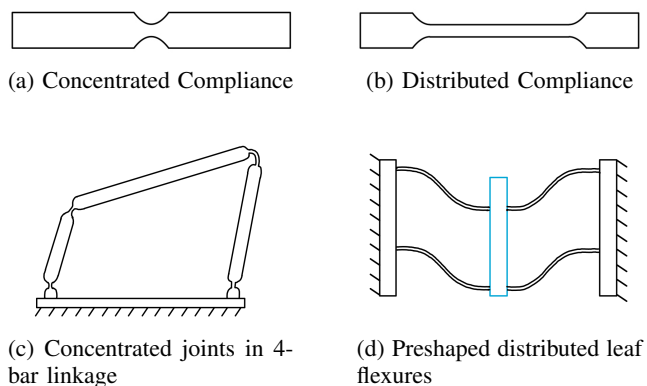


Fig. 2: Difference in concentrated and distributed compliance

By using these basics, different types of compliant hinges and joints have been designed so that it can be used for various robotic features. These hinges all have different characteristics such as range of motion and on- and off-axis stiffness [18]. A visualisation of some of these hinges can be found in Figure 3. Another configuration of a concentrated compliant hinge is that in the technique of origami mechanisms. Origami is the Japanese art of folding paper and this technique can be used in mechanisms to solve specific problems [19]. Described by the term

'kinetic origami', it refers to using this Japanese technique as a model that exhibits a mechanical motion [20]. A concentrated hinge can be used along the length of a rigid structure to create a crease around which the material can bend, thus creating the origami folding characteristics.

A bistable mechanism is another interesting composition of compliant mechanisms. This type of mechanism has, within a certain range of motion, two stable equilibrium positions. This could easily be created with the use of compliant mechanisms because of the flexible members and are useful in applications such as a bistable light switch or microdiaphragm valves [21, 22]. Bistable mechanisms could also be used to switch between two different states of stiffness, which could be an important fundamental for variable stiffness robotic applications [23].

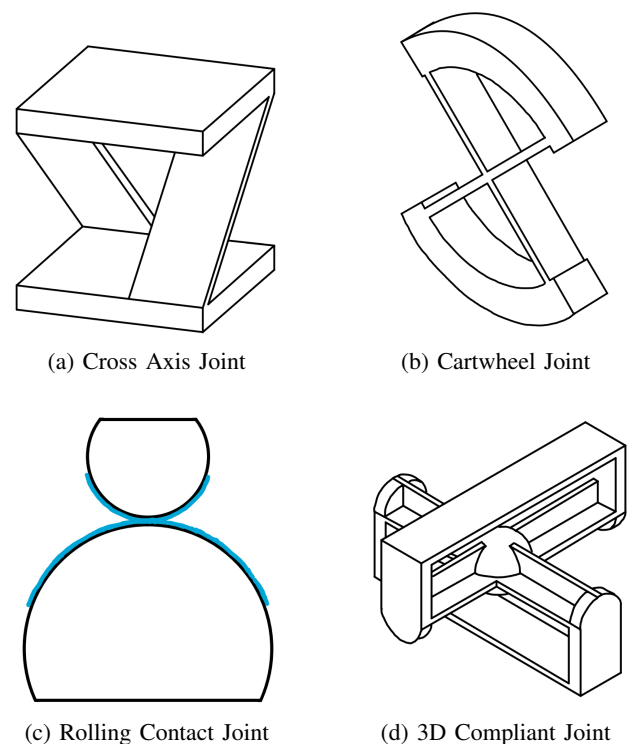


Fig. 3: Different compliant joints visualised [18]

The design and analysis of compliant mechanisms is relatively difficult, because of the numerous complex design possibilities and unusual motion characteristics. But this process gets less challenging with the use of three approaches [16]: Finite Element Analysis (FEA), Topology Optimization and Pseudo-Rigid-Body Models (PRBM). FEA is the most used method because of the conventional and commercial way to analyse the non-linear deflections and is also useful for the wide range of application areas for which compliant mechanisms can be used. Topology Optimization is known for the improving of the performance of the compliant mechanism. It can be used to optimize the desired actuation output, the weight of the mechanism or create the an optimal design between two

design requirements. *PRBM* makes use of analysing the mechanism with conventional rotational joints with springs attached to them, instead of the compliant hinges. By strategically place the joints and properly sized springs in the model, it is possible to achieve high accuracy into the nonlinear range. A visualisation is given in Figure 4. A PRBM is often used in the beginning of the design phase in order to quickly evaluate iterations, because conventional methods in mechanism design can be utilized, allowing for easy visualization of motions.

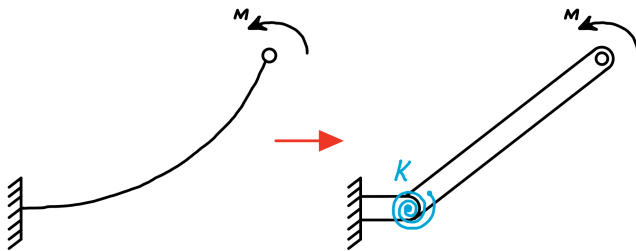


Fig. 4: Example of a PRBM: Simulating the leaf spring as a traditional mechanism with a spring on its joint

Compliant mechanisms and its joints are the basis for numerous mechanisms and application areas. By reconfiguring the flexible members or choosing different types of hinges in series or parallel, the working principle can change drastically. With the use of a PRBM and changing hinges a set of pliers has been developed [24], which is an excellent example of a general compliant mechanism. This kind of methodology is also used for two dimensional micro-electromechanical systems (MEMS) to create micro grippers, actuation methods or energy harvesting mechanisms [25, 26]. And by reconfiguring the mechanism, three dimensional structures can be developed such as joints, shape morphing lattices [27] or surgical applications [28].

To evaluate the state-of-the-art compliant mechanism used in flexible robotics, it is important to split the different mechanisms up in the three categories: General Compliant Mechanisms, Origami Robotics and Continuum Robotics. The first section will look into the mechanisms consisting of the pure use of compliant joints and hinges, such as the pliers or generic two dimensional structures. The second and third sections are subcategories as they use the basic fundamentals of compliant mechanisms to create a different characteristic and output. These are the continuum robotics, as they use compliant joints to create their flexible body but in the literature has many applications that it is worth mentioning it separately, and origami mechanisms as they use concentrated compliance to create a characteristic that is not easily achievable by the general compliance.

A good thing to mention is the fact that the terms General Compliant Mechanisms, Origami Mechanisms and Continuum Robotics are not separate disciplines but are closely related. As visualised in Figure 5, both origami mechanisms and continuum robotics make use of the general compliant mechanisms. This is the case because the

joints of this field could be arranged in a way to create the mechanisms falling under the other two terms as described in the previous paragraph. Moreover, origami mechanisms could also be used in continuum robotics by designing the compliant body (Figure 7) out of origami hinges and creases to create the desired characteristics.

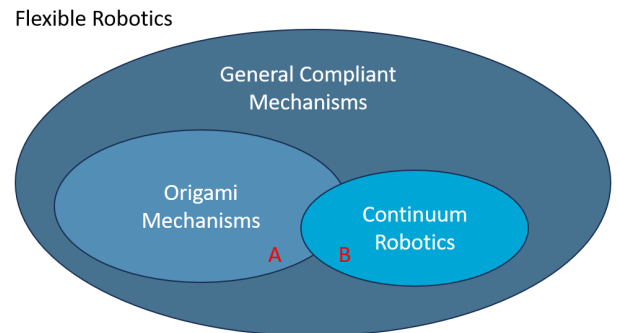


Fig. 5: The relation between all the subcategories used in Flexible Robotics

A. General Compliant Mechanisms

Under the general compliant mechanisms fall the mechanisms that use the basic joints or flexures to create a, mostly, two dimensional mechanism. A good example is the compliant robotic leg for small locomotion found in [29]. The mechanism makes use of a distributed kind of flexure as the bottom of a foot and with a rotation motor it is actuated to following a walking motion. It is essentially the same as a path generator such as the Jansen Linkage, which is a two dimensional walking mechanism to create a smooth walking motion by combining a circular and linear movement in a single mechanism. The aim of such a mechanism is to mimic a trajectory of a specific point in the mechanism to a desired output. Megaro (et al., 2017) [30] describes making this Jansen Linkage into a compliant version for the use of animatronics. The paper also talks about the design of a fully compliant operational hand, but the actuation method is again not compliant but with the use of hand or motor actuation. [31] developed a compliant foot and ankle mechanism to be placed in a prosthetic leg. The ankle is made out of a rotational joint and is actuated by the person itself when the foot touches the ground while walking, it is a passive compliant mechanism.

While these examples show the potential of compliant mechanisms in prosthesis, it can also be used to lower vibrations produced by a 3 degree of freedom (DoF) robotic arm [32]. The robotic arm itself is not compliant, but it is interesting to see how the compliant mechanism allows rotation around the three axis and can lower vibrations in that way.

Then there is also research performed in the direction of compliant grippers without the use of soft robotics. The main motivation for these application is the need for grabbing objects in challenging environment, rather than

fragile ones. The gripper described in [33] makes use of a concentrated compliant hinge mechanism for the two legs of the gripper. While the gripper is an excellent example of how to use compliant mechanisms, the mechanism is actuated with a linear actuator which is not compliant. In contrast, the gripper described in [34] is developed for micro and nano applications and uses a compliant piezoelectric stack to actuate it.

B. Origami Robotics

Origami is another branch of compliant mechanisms that could be used in flexible robotics. Origami is a mechanical structure that originated from the Japanese method of folding paper with the purpose that it was suitable for mechanical application. It involves using concentrated joints, like creases in the paper, to produce three dimensional shapes from a two dimensional sheet [35]. An illustration of an example of an origami configuration can be found in Figure 6. Bistable mechanisms are also used with origami to create multiple stages a mechanism could be in. These structures are called Miura and Waterbomb origami [36], with a variant that combines multiple of these origami to create a multistable mechanism. Applications for this technique range from biomedical devices, space application to precision actuation mechanisms and foldable and stretchable electronics.

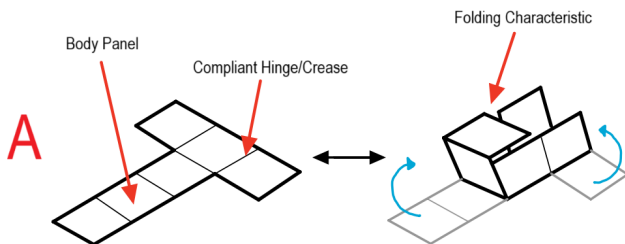


Fig. 6: Example of an origami structure

Different examples of origami used as compliant mechanisms in flexible robots exist in the literature, ranging from grippers to continuum like robots. The origami used for grippers is difficult to design because of the complex mechanism that couples the input and output. By squeezing down on one side of the mechanism, the other side folds drastically to create a gripping motion [37]. The continuum like robot replaces the flexure like body of the mechanism mentioned in the previous section and replaces it with an origami structure that can rotate around the x- and y-axis and twist around its length (the z-axis). With the use of a cable driven mechanism, the robot is able to bend itself in all direction like a conventional continuum robot can. In addition to this, the robot has three smaller continuum origami bodies on the end with which it can grasp fragile objects.

Within a different field of robotics, there is also an origami flexible robot that can navigate through the esophagus towards to stomach while collapsed and expand when it arrives [38]. With the use of its shape, the fluids in the

stomach and an external magnet it is able to walk along the stomach wall to the spot where it needs to be. The mechanism is fully degradable and this process will start once it arrives in the stomach and is fully complete long after the purpose has been served.

C. Continuum Robotics

These type of robotics do not contain rigid links and conventional rotational joints but instead use structures that bend continuously along there length via elastic deformation [15]. Robots incorporating continuum mechanisms can navigate and manipulate within concealed and confined spaces while adjusting to the curved paths of the environment. A cable driven method is the most used actuation method for such mechanisms. The use of a cables to drive the mechanisms is called extrinsic and makes use of the fact that if one side of the structure is shortened (by pulling on the cable) that it bends towards that side and vice versa. An illustration is given in Figure 7.

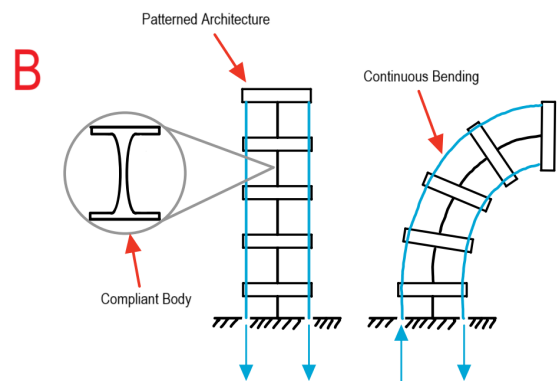


Fig. 7: Basic principle of continuum robots with a compliant joint

The basic version is described by Wei Li et al. [39] where a simple compliant body is actuated using 2 wires in a two dimensional plane. By changing the internal structure of the compliant mechanism, the way of bending it changed slightly. This type of mechanisms is mostly used in application for locomotion and grasping. For example, continuum robotics is used in the compliant body of a robotic fish [40, 41] to steer it in the correct direction. Instead of using multiple cables, the mechanism uses a continuous cable that is actuated with a motor to increase and decrease the cable on both sides of the fish. Another use of continuum robots is popular in the medical world. It can especially be used for minimal invasive surgery, because of the large flexibility. It is for example used in an articulated endoluminal forceps inside an endoscope for the removal of cancer tissues [42]. The mechanism uses 4 cables to be bend in all directions except around its own axis, which creates a very big range of motion to reach different kinds of locations in the body. This mechanism is also described by Berthet-Rayne et al. [43]. Bandara et al. [44] also makes use of cable driven actuation inside

surgical forceps, but here the forceps themselves can bend continuously around the base instead of the base itself. The cables push against one side of the forceps in order for it to make it bend, but the bending radii is a lot less than the previously mentioned surgical tool.

A different kind of cable driven compliant arm is the arm described in [45]. This arm has a compliant body made of flexure joints, which have a large range of motion and low stiffness. The mechanism is again actuated with 2 wires, but it has a different method of navigating tiny spaces. The last mentioned continuum robots would jump back to their original position once the tension is released from the wires. That is also the case for this mechanism, but it uses the phenomenon called Underactuation. Instead of the robot not wanting to touch the environment in order to prevent damage on the environment or the robot itself, this mechanism is able the anchor itself against the walls of the environment. If the tension is removed from the cables, it will keep its shape the environment gave it. If the robot is pushed forward, the front can be steered again, while the rest of the body is able to adjust itself to the environment. But this is of course not possible in every situation.

And there also exist a variant on continuum robots that do not make use of a cable driven mechanism, but make use of flexible corrugated tubes that make up the body [46]. It makes use of three of these tubes in the shapes of a triangle and that can move up and down with the use of a geared motor. If one of the tubes is elongated, it will bend in that direction. And another version makes use of compliant springs as joints in the body, but the actuation method has not been mentioned. It is purely experimental without a direct application area, so it has been actuated by hand for different experiments.

D. Challenges for Compliant Mechanisms in Flexible Robotics

From the found literature and the summary in the previous subsections a numerous of challenges were observed and mentioned below.

One of the key features of flexible robots is its compliant design which gives it the ability to work in all kinds of different environments. And while all the mentioned applications show fundamentals of working principles, there is one aspect of the robots where an opportunity lies and that is on the actuation side of the mechanisms. Compliant mechanisms, also in the form of origami and continuum robots, have proven themselves on multiple aspects to be useful in different kinds of applications, but if the actuation method is not compliant it cannot fully serve its purpose. While using a cable driven mechanism or traditional electric motor, the applications still benefit from the added advantages of the compliant body such as the the lubrication that can be left out, no particle production and a high repeatability. But when looking into the next steps for flexible robotics, it is of interest to solve these problems of the actuators producing particles, need lubrication and are in need of big assembly tasks. So to make sure future

robotics could be deployed in multiple environments, it is of interest to look into a compliant kind of actuators. But what are compliant actuators?

IV. SMART MATERIAL ACTUATION FOR COMPLIANT MECHANISMS

Compliant actuators are the exact opposite of a non-compliant actuator, which can be defined by a stiff actuator which is a device that is able to move to a specific position and stay there whatever the external forces are on the actuator [47]. A compliant actuator will allow deviation from the equilibrium position under external loads, but this can be minimized. The most conventional actuators for these purposes are the hydraulic and pneumatic actuators used in soft robotics, which can easily be found in the literature. Looking further into the recent advances in compliant actuators shows the use of smart materials for this purpose.

Smart material actuators are devices that have embodied intelligence, which are internal specification with unique properties to generate a mechanical motion or force while stimulated with the correct, external, triggers like an electric or magnetic field, temperature change, light or pH. They are often referred to as smart because they have the ability to alter their properties in a controllable manner which is also reversible. The most well known smart materials are shape morphing materials, electro- and magnetostrictive materials and thermoelectric materials. The smart materials actuated by light or pH are not of interest because of the need for the robot to work in challenging environments where this is difficult to implement. This has also been confirmed by the literature search where no examples of these stimuli have been found in combination with compliant mechanisms or flexible robotics. The others will be discussed in the next sections.

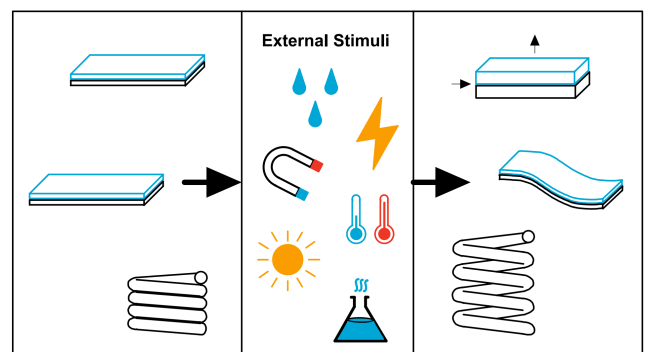


Fig. 8: The influence of different stimuli on smart materials

A. Shape Memory Materials

Shape memory materials are characterized by their capability to regain their initial shape after undergoing, what seems like, plastic deformation after the correct external stimuli has been applied [48]. This phenomenon is called the shape memory effect (SME) and this can be found in two different types: Shape memory alloys (SMAs) and shape memory polymers (SMPs). An example of both types of materials can be found in Figure 8.

The first SMAs that exhibited this effect were found in Ti-Ni and Cu-Al-Ni alloys in 1963 [49] and could recover their shape completely when heated above a certain temperature. The alloys undergo a thermoelastic martensitic transformation and shift their shape with a temperature change or in other words a thermal activation. But it is also possible to activate these alloys with the use of an electric current [50]. By running this current through a material that generates resistive heating, it counts as a change of heat and the SME is set in motion. An advanced of this is that with the use of an electric current the control of the temperature is more accurate and more rapid.

The use of SMAs have a few advantages apart from the fact that it could be used as a compliant actuator. SMAs could undergo large deformations and could still go back to their original shape, meaning they could be ideal for the use in macro robotics. SMAs have good mechanical properties which includes high strength and durability, which results in a relative large power density. The actuation time of SMAs depends on how quickly the temperature can change, which depends on its input values. The downsides of SMAs is that they are relatively expensive and experience some creep, which is the slow deformation under constant stress. Additionally they have a big power consumption, which could be solved by integrating a SMA actuator with a multi-stable structure [51], because remaining in either stable states would result in no input power.

The use of SMAs in combination with compliant mechanisms are mostly fundamentally explored, meaning that underlying principle of a possible robotic feature is examined thoroughly. But there are little to no fully developed robots mentioned in the literature for the recommended application areas. An example of this is the use of an origami hinge with the use of a SMA [52] that ensures the automatic bending of a certain origami section. This proves the ability of SMAs with working with origami mechanisms and potentially other compliant variations. The same counts for the ability of SMAs to bend metal plates in order to manipulate a structure, with an example for automatic ventilation shafts in buildings [53]. Rigid compliant linkages with concentrated or distributed body parts, with application opportunities in micro-scale manipulation devices, biomedical devices and metastructures, are also proven to have been actuated using a thermally driven wire [54]. And next to that it is a promising technique for the use of locomotion combined with compliant bistable mechanisms to lower the needed power [55].

Along the lines of origami, there are also applications of fundamentals for deployable structures. SMAs are used for actuator to create a 180° bend from a 0° starting point and are enveloped by a polydimethylsiloxane (PDMS) elastomer that keeps the internals together [56]. But the most interesting part is the use of a fusible alloy (FA) that can shift its state under thermal activation. This means that the structure can change its stiffness between actuation to carry loads.

SMPs are closely related to SMAs, because they have the ability to temporarily change their shape when exposed to an external stimulus as well but in a polymer form. The main applications lie in various fields that are in need for their reversible shape-changing capabilities. This can be seen in the origami field of compliant mechanisms where SMPs are used to bend a hinge between two rigid panels with the use of active composites where the shape memory polymer fibers are directly printed into the elastomeric matrix [57]. SMPs are also of use in the twistable origami and kirigami where SMPs are used to actuate the structure entirely or for example in a locomotion robot where the legs are assembled out of a two dimensional sheet [58].

B. Electro- and Magnetostrictive Materials

Electrostrictive materials are a type of smart material that undergo mechanical deformation in response to an applied electric field. This deformation is caused by the rearrangement of the internal structure of the material's molecules in the presence of an electric field [59]. Electrostriction is the phenomenon where a material changes its shape in response to an electric field, and this effect is reversible. The same effect is possible when certain materials are exposed to a magnetic field which are called magnetostrictive materials.

There are multiple subcategories that fall under these terms. The first subcategory is the piezoelectric materials, which consist mostly of crystals, ceramics or polymers that exhibit the piezoelectric effect. This effect is described by the ability to generate an electric charge in response to mechanical stress or deformation, or vice versa. If the electric field is switched off, the material will return to its original state. A representation of this working principle can be found in Figure 9. A multiple of these materials together in a tower-like configuration is known as a piezoelectric stack and has applications for actuation, energy harvesting and sensors because of the straight line actuation. Within the field of compliant mechanisms the piezoelectric stack is used for lockable shape morphing lattices for airplane wings [60, 61], but also compliant amplifiers [62, 61] to boost the characteristics of the stack. One of the disadvantages of the piezoelectric stack is that it has a limited displacement range, which hardly exceeds 100 μ m [63]. But this does make the piezoelectric stack ideal for applications such as micro grippers [64, 65] and

slightly large surgical forceps [66]. Other advantage of the stack are a high force output, precision control possibilities and their compact size.

The second subcategory that is being used for compliant mechanism are the electroactive polymers (EAPs) and the magnetoactive elastomers (MAEs), which are both types of smart materials that undergo mechanical deformation as a responds on an external stimuli. But the first reacts to an applied electric field and the other an applied magnetic field. Both materials have application areas in soft robotics, vibration damping, sensors and actuators. Dielectric elastomers are a class of electroactive polymers which have an elastomeric material sandwiched between compliant electrodes. Due to the electrostatic forces between the layers, the material experiences a change in thickness or area.

EAPs have the advantage that they have a large deformation range and are lightweight, but they require a high voltage, are not that durable over a large number of actuations and have a complex control system. For MAEs it is roughly the same, although they have a more limited operation deflection but they are mechanically tunable. Think of the stiffness and damping.

The use of these materials for compliant mechanisms has more capabilities than the piezoelectric stack. They are mostly used in soft robotic applications, but have fundamental applications with compliant mechanisms. One of the ways to apply MAEs is in combination with a bistable mechanism [67]. Due to the applied magnetic field, the bistable could be triggered into the second stable position and back saving energy. And the application of EAPs in microposition stages is also validated [68]. Here, the EAP is rigidly connected but could twist up and down when an electric field is applied. As has been said this is a fundamental piece of research for a precision z-stage, but this could indicate for the possibilities of adding EAPs in robotic applications such as locomotion or stiffness changing robotic arms. EAPs are already added to numerous applications on their own, not necessarily with compliant mechanism. These applications range from a flapping robotic fly, a small gripper and a multi-joint robotic finger which uses traditional joints [69].

As mentioned in the beginning of this chapter, there are multiple other smart materials such as the hydrogels and rheological fluid actuators. While these have not been found in the literature in combination with compliant mechanisms, it is important to mention these techniques as possibilities when looking into the future of robotics. They could have similar basic functionalities as described in Figure 9 such as a hydrogel could absorb and retain a significant amount of water more on the top of the material than at the bottom to make sure a bend is created. For the rheological fluid actuators, it is possible to create an application with variable stiffness and could lock the material in place ones the viscosity of the material has been shifted. However, these materials are not commonly

used for flexible robotics in combination with compliant mechanisms as far as the literature goes.

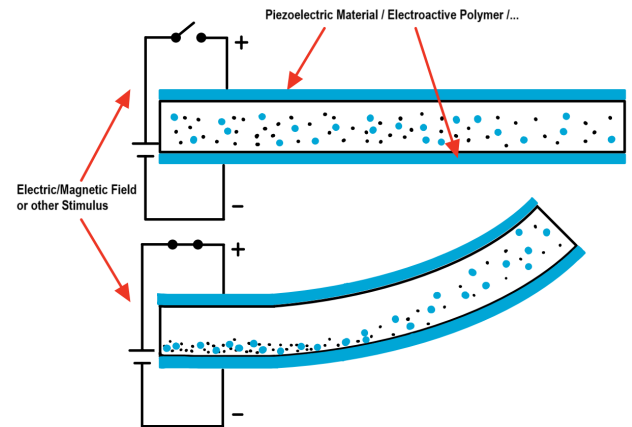


Fig. 9: Example of piezoelectric material or electroactive polymers in an application

C. Hybrid Use of Smart Materials

Another recent innovation within the world of smart material actuation for compliant mechanism is the hybrid systems. This means that multiple different smart material actuators will be used to create, or, other properties or enhance a property. The combination of shape morphing alloys with piezoelectric material could lead to the creation of a better shape morphing wing for unmanned aerial vehicles [70]. Or the characteristics of dielectric and magnetoactive elastomers could be combined in a single mechanism to create multiple bending possibilities, as visualised in Figure 10. An origami mechanism could bend a certain way when an electric field is applied, but can behave completely different the external stimulus switched to a magnetic field. While the literature about this topic is still scarce in the field of compliant mechanisms, it could be of great value for future applications.

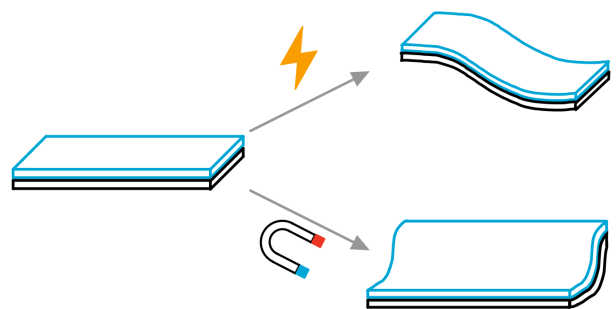


Fig. 10: A part could have different reactions to multiple stimuli to satisfy multiple functions

V. A WAY FORWARD IN FLEXIBLE ROBOTICS

To create a comprehensive overview of the found literature and to make a potential literature gap visible, a matrix has been made to highlight most of the technologies used between the flexible robotics and smart material actuated compliant mechanisms field. This table can be found in [Table I](#). When looking in the matrix, the first visible literature gap is that of the continuum robotics with the use of smart material actuators. The most recent and most used technology for continuum robotics is the cable driven actuator and in the literature no real examples of the use of smart materials is present. The second difference is the fact that the piezoelectric stack has not been used for origami mechanisms. This is due to the fact that this actuator has a short stroke length and is mostly used in micro and nano applications, while origami mechanisms mostly need a larger stroke. And to further elaborate on the matrix, the next subsection contains recommendations for possible ways forward in the flexible robotics field. The recommendations are explained according to the respective underlying compliant principles.

A. Recommendations

1) *General Compliant Mechanisms:* Basic compliant mechanisms, concentrated or distributed, are already greatly researched and there is a good understanding of what is possible. But for flexible robotics with smart material actuation, there is still room for improvement. By combining the available techniques, it would be very interesting to combine a smart material actuated bistable mechanisms into a variable stiffness mechanisms to apply in robotic arms. Or having electroactive polymers take control of new path generators for locomotion. And while the flexible robots with compliant mechanisms and actuation are mainly focused on the micro and nano world for MEMS and micro grippers, it could be of interest to test out the amplification mechanisms to create application that are scaled upwards instead of down. It is convenient because the piezoelectric stack has a very small stroke actuation, but maybe there are possibilities to implement them in compliant macro grippers for space applications. Another great technology that has been mentioned in [56] is the use of fusible alloys in stiffness changing applications. These fusible alloys can shift phase because of their very low melting point and essentially could 'lock' joints in place that are submerged in this alloy.

With the current advances in 3D printing, which is already the most used manufacturing tool for prototypes and even real application, it could be of interest to look into assembling the actuation method directly into the mechanism while it is still printing. An advantage would be the low assembly time and it creates opportunities to make the structure more compact. Furthermore it would be better to control because the assembly technique is more predictable and overall it would be more efficient and create more versatile robotic movements.

2) *Continuum Robotics:* Continuum robotics is an outstanding subcategory of compliant mechanism with numerous application field such as locomotion and gripping for minimally invasive surgery, soft grippers and manipulators and the navigation of challenging spaces. But the actuation methods are largely cable driven or provided by an electric motor. While the literature does not state the use of smart material actuators with continuum robotics specifically, there are recommendations that could be made. Zhang et al. [76] describes a mechanism that makes use of a hybrid design using both pneumatic actuators as cable driven ones to actuate a continuum robot. But he also admits in the conclusion that by using smart material actuators such as shape memory alloys could decrease complexity and further increase the miniaturization of the mechanism.

All the different smart material actuators covered in this paper could be of use in continuum robotics. Applications could range from fully compliant robotic arms, either with compliant joints or origami structures, to the use for more complex locomotion or variable stiffness arms.

3) *Origami Mechanisms:* The main advantages of origami mechanisms is that they have a low price point in terms of manufacturing and they are lightweight and compact. These mechanisms have already numerous applications for space exploration, such as the James Webb telescope, medical surgery devices, in the automotive industry in the form of an airbag and possible application in the industrial industry. But for the use in flexible robotics in combination with smart material actuation, it shows that the fundamentals are already in place. All the different types of smart material actuators have been proven to bend and twist the origami structure to their desired position. The only actuator that has not been implemented is the piezoelectric stack due to its minimal stroke length.

These origami structures and actuation types could be implemented in (continuum) robotic arms. It would be possible to reconfigure the mechanism to use shape memory alloys as a way to implement a variable stiffness mechanism into it. Or the electrostrictive materials could be used with origami to create macro grippers as this would be possible due to their large actuation angle. Different types of locomotion, which has previously been done in worm-like structures using shape memory alloys, would be possible to create a walking like motion. Hybrid actuation methods could help with making the robotic applications more versatile. While under the influence of an electric field, the mechanisms could be used for locomotion while by using a magnetic stimulus it could change the structure so it can be used for grabbing objects.

B. Emerging Technologies

With the use of the new modeling techniques available this day and age, the non-linear behaviours of compliant mechanisms and smart material actuators could be combined to create a better understanding and eventually robotic applications. The current industrial market asks

	General Compliant Mechanisms	Origami Mechanisms	Continuum Robotics
Shape Memory Materials	Deployable Structure [56] XY Precision Stage [71] Rigid Body Mechanisms [54]	Variable Stiffness Hinges [72] Normal Hinge Mechanisms [53, 73] Twistable Origami [74] Ventilation Systems [52]	There are no examples in literature , but there are numerous of recommendations that could be of value. Such as locomotion, gripping applications and robotic manipulators in combination with smart materials.
Electro- and Magnetostrictive Polymers	Z Moving Stage [68] Bistable Mechanisms [67] Grippers [69] A lot of Soft Robotics	Bistable Origami Mechanisms [67] Origami Hinges [73]	
Piezoelectric Stack	Micro Grippers [64, 65] Medical Applications [65] Shape Morphing Lattices [60] Amplification Mechanisms [62, 61]	-	
Hybrid Systems	Shape Morphing Lattices [70]	Deployable Structures [75]	

TABLE I: The different combinations of compliant mechanisms and smart actuators in literature

for more and more compliant mechanisms due to the challenging environments robots have to work in. This could be the aerospace, offshore and maritime industry or precision mechanisms operating in vacuum. These techniques are FEA, PRBM and Topology Optimization that keep continuing to improve each year. Secondly, the rising technology of 3D and 4D printing creates more opportunity for complex compliant structures. Think of printing the smart material actuator inside the material itself to create a more rigid structure that is better to predict and control.

VI. CONCLUSION

The potential enhancement of future flexible robots through the integration of smart material actuators instead of conventional actuation methods has been explored as a prospective opportunity. A thorough examination of the contemporary literature on compliant mechanisms in flexible robotics revealed a recurrent bottleneck in actuation processes. Commonly, these mechanisms were activated manually, employed electric motors, or were cable-driven. The introduction of a compliant actuation method was identified as a viable solution to tackle this bottleneck, rendering robots more adaptable for diverse applications in various working environments. Consequently, we proposed to shift the focus more towards investigating smart material actuators as a plausible means of addressing this challenge.

Smart material actuators for compliant mechanisms have been investigated up to a similar point as the literature of compliant mechanisms themselves. Different materials like shape memory materials, the electro- and magnetostrictive materials and the hybrid solutions all have been evaluated to a certain extend where it can be concluded that they are capable of working with compliant mechanisms.

However, we came to the conclusion that this field is lacking that, while the fundamentals of both innovations have proven to work great, there are not a lot of papers working on actually implementing these techniques together in real life industrial applications.

The recommendations range from focusing on a robotic compliant continuum manipulator actuated with smart materials for applications in challenging environments or locomotion implementations. However, this step towards

more complex and bigger applications is not something to take in one go. While there are papers that prove certain smart materials can actuate a very simple compliant structure, there are a lot of intermediate steps towards the big picture. It could be of great value to look into variable stiffness compliant mechanisms actuated by smart materials instead by the human hand, or the use of smart material actuated origami in continuum robots before looking for the straight implementation of the full robotic arm into the aerospace industry. Smaller applications, such as the use of fusible alloys or even the use of piezoelectric stacks in macro mechanisms, could already be of great value towards the future in robotics.

REFERENCES

- [1] Alan Winfield. *Robotics: A Very Short Introduction*. Oxford University Press, Sept. 2012. ISBN: 9780199695980.
- [2] Elena Garcia et al. “The evolution of robotics research”. In: *IEEE Robotics & Automation Magazine* 14.1 (2007), pp. 90–103.
- [3] D Arulkirubakaran et al. “Evolution of Industrial Robots During Mid of Nineteenth Century–Beginning of Twentieth Century—A Review”. In: *Recent Advances in Materials and Modern Manufacturing: Select Proceedings of ICAMMM 2021* (2022), pp. 143–154.
- [4] Ying Yang et al. “Flexible actuators for soft robotics”. In: *Advanced Intelligent Systems* 2.1 (2020), p. 1900077.
- [5] George M Whitesides. “Soft robotics”. In: *Angewandte Chemie International Edition* 57.16 (2018), pp. 4258–4273.
- [6] Carmel Majidi. “Soft robotics: a perspective—current trends and prospects for the future”. In: *Soft robotics* 1.1 (2014), pp. 5–11.
- [7] James Walker et al. “Soft robotics: A review of recent developments of pneumatic soft actuators”. In: *Actuators*. Vol. 9. 1. MDPI. 2020, p. 3.
- [8] Carmel Majidi. “Soft-matter engineering for soft robotics”. In: *Advanced Materials Technologies* 4.2 (2019), p. 1800477.

- [9] Ela Sachyani Keneth et al. “3D printing materials for soft robotics”. In: *Advanced Materials* 33.19 (2021), p. 2003387.
- [10] Ryuma Niiyama. “Soft Actuation and Compliant Mechanisms in Humanoid Robots”. In: *Current Robotics Reports* 3.3 (2022), pp. 111–117.
- [11] Cecilia Laschi, Barbara Mazzolai, and Matteo Cianchetti. “Soft robotics: Technologies and systems pushing the boundaries of robot abilities”. In: *Science robotics* 1.1 (2016), eaah3690.
- [12] Yee Ling Yap, Swee Leong Sing, and Wai Yee Yeong. “A review of 3D printing processes and materials for soft robotics”. In: *Rapid Prototyping Journal* 26.8 (2020), pp. 1345–1361.
- [13] Panagiotis Polygerinos et al. “Soft robotics: Review of fluid-driven intrinsically soft devices; manufacturing, sensing, control, and applications in human-robot interaction”. In: *Advanced Engineering Materials* 19.12 (2017), p. 1700016.
- [14] Oncay Yasa et al. “An Overview of Soft Robotics”. In: *Annual Review of Control, Robotics, and Autonomous Systems* 6 (2023), pp. 1–29.
- [15] Graham Robinson and J Bruce C Davies. “Continuum robots-a state of the art”. In: *Proceedings 1999 IEEE international conference on robotics and automation (Cat. No. 99CH36288C)*. Vol. 4. IEEE. 1999, pp. 2849–2854.
- [16] Larry L Howell. “Compliant mechanisms”. In: *21st Century Kinematics: The 2012 NSF Workshop*. Springer. 2013, pp. 189–216.
- [17] Jordan Cormack et al. “Comparison of Concentrated and Distributed Compliant Elements in a 3D Printed Gripper”. In: *Annual Conference Towards Autonomous Robotic Systems*. Springer. 2021, pp. 193–197.
- [18] D Farhadi Machekposhti, N Tolou, and JL Herder. “A review on compliant joints and rigid-body constant velocity universal joints toward the design of compliant homokinetic couplings”. In: *Journal of Mechanical Design* 137.3 (2015), p. 032301.
- [19] Erik D Demaine and Joseph O’Rourke. *Geometric folding algorithms: linkages, origami, polyhedra*. Cambridge university press, 2007.
- [20] HC Greenberg et al. “Identifying links between origami and compliant mechanisms”. In: *Mechanical Sciences* 2.2 (2011), pp. 217–225.
- [21] Brian D Jensen and Larry L Howell. “Identification of compliant pseudo-rigid-body four-link mechanism configurations resulting in bistable behavior”. In: *J. Mech. Des.* 125.4 (2003), pp. 701–708.
- [22] WK Schomburg and C Goll. “Design optimization of bistable microdiaphragm valves”. In: *Sensors and Actuators A: Physical* 64.3 (1998), pp. 259–264.
- [23] Sam Shimohara, Ryan H Lee, and Jonathan B Hopkins. “Compliant mechanisms that achieve binary stiffness along multiple degrees of freedom”. In: *Journal of Composite Materials* 57.4 (2023), pp. 645–657.
- [24] Larry L Howell and Ashok Midha. “A method for the design of compliant mechanisms with small-length flexural pivots”. In: (1994).
- [25] Sridhar Kota et al. “Design of compliant mechanisms: applications to MEMS”. In: *Analog integrated circuits and signal processing* 29 (2001), pp. 7–15.
- [26] Haitong Liang, Guangbo Hao, and Oskar Z Olaszewski. “A review on vibration-based piezoelectric energy harvesting from the aspect of compliant mechanisms”. In: *Sensors and Actuators A: Physical* 331 (2021), p. 112743.
- [27] SP Jagtap, BB Deshmukh, and S Pardeshi. “Applications of compliant mechanism in today’s world—A review”. In: *Journal of physics: conference series*. Vol. 1969. 1. IOP Publishing. 2021, p. 012013.
- [28] Theodosia Lourdes Thomas et al. “Surgical applications of compliant mechanisms: A review”. In: *Journal of mechanisms and robotics* 13.2 (2021), p. 020801.
- [29] Huai Huang, Yangzhi Chen, and Yueling Lv. “A Novel Robot Leg Designed by Compliant Mechanism”. In: *Intelligent Robotics and Applications: 7th International Conference, ICIRA 2014, Guangzhou, China, December 17-20, 2014, Proceedings, Part I* 7. Springer. 2014, pp. 204–213.
- [30] Vittorio Megaro et al. “A computational design tool for compliant mechanisms.” In: *ACM Trans. Graph.* 36.4 (2017), pp. 82–1.
- [31] Tan Thang Nguyen et al. “Evaluation of structural behaviour of a novel compliant prosthetic ankle-foot”. In: *2017 International Conference on Mechanical, System and Control Engineering (ICMSC)*. IEEE. 2017, pp. 58–62.
- [32] Mohammad Zubair and Seul Jung. “Design and Analysis of Flexure Joint for a Flexible Robotic Arm”. In: *2022 13th Asian Control Conference (ASCC)*. IEEE. 2022, pp. 2201–2205.
- [33] Timothy Vittor et al. “A flexible robotic gripper for automation of assembly tasks: A technology study on a gripper for operation in shared human environments”. In: *2011 IEEE International Symposium on Assembly and Manufacturing (ISAM)*. IEEE. 2011, pp. 1–6.
- [34] Michael Goldfarb and Nikola Celanovic. “A flexure-based gripper for small-scale manipulation”. In: *Robotica* 17.2 (1999), pp. 181–187.
- [35] Cheng Lv et al. “Origami based mechanical metamaterials”. In: *Scientific reports* 4.1 (2014), p. 5979.
- [36] Yinding Chi et al. “Bistable and multistable actuators for soft robots: Structures, materials, and functionalities”. In: *Advanced Materials* 34.19 (2022), p. 2110384.

- [37] Jie Liu et al. “Nonlinear topology optimization design and gripping tests of a novel origami chomper-based flexible gripper”. In: (2023).
- [38] Shuhei Miyashita et al. “Ingestible, controllable, and degradable origami robot for patching stomach wounds”. In: *2016 IEEE international conference on robotics and automation (ICRA)*. IEEE. 2016, pp. 909–916.
- [39] Wei Li et al. “Design and Modelling of A Spring-Like Continuum Joint with Variable Pitch for Endoluminal Surgery”. In: *2022 IEEE/RSJ International Conference on Intelligent Robots and Systems (IROS)*. IEEE. 2022, pp. 41–47.
- [40] Yong Zhong and Ruxu Du. “Design and Implementation of a Novel Robot Fish with Active and Compliant Propulsion Mechanism.” In: *Robotics: Science and Systems*. Vol. 12. 2016.
- [41] Liming Ge et al. “Design and analysis of wire-driven tail fin for bionic underwater glider”. In: *Ocean Engineering* 286 (2023), p. 115460.
- [42] Keisuke Osawa et al. “2.5-mm articulated endoluminal forceps using a compliant mechanism”. In: *International Journal of Computer Assisted Radiology and Surgery* 18.1 (2023), pp. 1–8.
- [43] Pierre Berthet-Rayne et al. “Rolling-joint design optimization for tendon driven snake-like surgical robots”. In: *2018 IEEE/RSJ international conference on intelligent robots and systems (IROS)*. IEEE. 2018, pp. 4964–4971.
- [44] DSV Bandara et al. “3.5 mm compliant robotic surgical forceps with 4 DOF: design and performance evaluation”. In: *Advanced Robotics* 37.4 (2023), pp. 270–280.
- [45] Sergio Jainandunsing et al. “Design of a compliant environmentally interactive snake-like manipulator”. In: *ROMANSY 21-Robot Design, Dynamics and Control: Proceedings of the 21st CISM-IFTOMM Symposium, June 20-23, Udine, Italy*. Springer. 2016, pp. 233–240.
- [46] Mingyuan Wang et al. “Design of a modular continuum robot with alterable compliance using tubular-actuation”. In: *2022 IEEE/RSJ International Conference on Intelligent Robots and Systems (IROS)*. IEEE. 2022, pp. 1923–1928.
- [47] Ronald Van Ham et al. “Compliant actuator designs”. In: *IEEE Robotics & Automation Magazine* 16.3 (2009), pp. 81–94.
- [48] WM Huang et al. “Shape memory materials”. In: *Materials today* 13.7-8 (2010), pp. 54–61.
- [49] T Tadaki, K Otsuka, and K Shimizu. “Shape memory alloys”. In: *Annual Review of Materials Science* 18.1 (1988), pp. 25–45.
- [50] François Schmitt et al. “Soft robots manufacturing: A review”. In: *Frontiers in Robotics and AI* 5 (2018), p. 84.
- [51] Silvestro Barbarino et al. “A review on shape memory alloys with applications to morphing aircraft”. In: *Smart materials and structures* 23.6 (2014), p. 063001.
- [52] Yudong Fang and Edwin A Peraza Hernandez. “Modeling and design optimization of shape memory alloy-enabled building skins for adaptive ventilation”. In: *Journal of Intelligent Material Systems and Structures* 33.16 (2022), pp. 2086–2105.
- [53] Zhenishbek Zhakypov and Jamie Paik. “Design methodology for constructing multimaterial origami robots and machines”. In: *IEEE Transactions on Robotics* 34.1 (2018), pp. 151–165.
- [54] Yudong Fang, Woo Rib Suh, and Edwin A Peraza Hernandez. “Parametric optimization of continuum mechanisms incorporating active material actuation”. In: *Sensors and Smart Structures Technologies for Civil, Mechanical, and Aerospace Systems 2020*. Vol. 11379. SPIE. 2020, pp. 227–236.
- [55] Lingda Meng et al. “A mechanically intelligent crawling robot driven by shape memory alloy and compliant bistable mechanism”. In: *Journal of Mechanisms and Robotics* 12.6 (2020), p. 061005.
- [56] Wei Wang, Hugo Rodrigue, and Sung-Hoon Ahn. “Deployable soft composite structures”. In: *Scientific reports* 6.1 (2016), p. 20869.
- [57] Qi Ge et al. “Active origami by 4D printing”. In: *Smart materials and structures* 23.9 (2014), p. 094007.
- [58] Samuel Felton et al. “A method for building self-folding machines”. In: *Science* 345.6197 (2014), pp. 644–646.
- [59] D Damjanovic and RE Newnham. “Electrostrictive and piezoelectric materials for actuator applications”. In: *Journal of intelligent material systems and structures* 3.2 (1992), pp. 190–208.
- [60] Yinjun Zhao et al. “A compliant-mechanism-based lockable prismatic joint for high-load morphing structures”. In: *Mechanism and Machine Theory* 178 (2022), p. 105083.
- [61] Tran Vy Khanh Vo et al. “Large-scale piezoelectric-based systems for more electric aircraft applications”. In: *Micromachines* 12.2 (2021), p. 140.
- [62] S Canfield and M Frecker. “Topology optimization of compliant mechanical amplifiers for piezoelectric actuators”. In: *Structural and Multidisciplinary Optimization* 20 (2000), pp. 269–279.
- [63] SB Shao et al. “Optimal design of the large stroke piezoelectric actuator using rhombic mechanism”. In: *Recent Advances in Structural Integrity Analysis—Proceedings of the International Congress (APCF/SIF-2014)*. Woodhead Publishing Oxford, UK. 2014, pp. 442–446.
- [64] Joël Agnus et al. “Description and performances of a four-degrees-of-freedom piezoelectric gripper”. In: *Proceedings of the IEEE International Symposium on Assembly and Task Planning, 2003*. IEEE. 2003, pp. 66–71.

- [65] Amr M El-Sayed et al. “Development of a micro-gripper using piezoelectric bimorphs”. In: *Sensors* 13.5 (2013), pp. 5826–5840.
- [66] David J Cappelleri and Mary I Frecker. “Optimal design of smart tools for minimally invasive surgery”. In: *Proceedings of Optimization in Industry II, Banff, Canada* 110 (1999).
- [67] Adrienne Crivaro et al. “Bistable compliant mechanism using magneto active elastomer actuation”. In: *Journal of Intelligent Material Systems and Structures* 27.15 (2016), pp. 2049–2061.
- [68] Rahim Mutlu, Gursel Alici, and Weihua Li. “A soft mechatronic microstage mechanism based on electroactive polymer actuators”. In: *IEEE/ASME Transactions on Mechatronics* 21.3 (2015), pp. 1467–1478.
- [69] Jung-Woo Sohn and Seung-Bok Choi. “Various robots made from piezoelectric materials and electroactive polymers: a review”. In: *Int. J. Mech. Syst. Eng.* 3.1 (2017), p. 122.
- [70] Alexander M Pankonien. “Smart Material Wing Morphing for Unmanned Aerial Vehicles.” PhD thesis. 2015.
- [71] Donghyun Hwang and Toshiro Higuchi. “A planar wobble motor with a XY compliant mechanism driven by shape memory alloy”. In: *IEEE/ASME Transactions on mechatronics* 21.1 (2015), pp. 302–315.
- [72] Yanlin Li et al. “Design and Analysis for Variable Stiffness of Memory Alloy Combined U-Shape Lamina Emergent Joint (Macu-Lej)”. In: *Available at SSRN 4143289* ().
- [73] EA Peraza Hernandez, Darren J Hartl, and Dimitris C Lagoudas. “Active origami”. In: *Active Origami* (2019).
- [74] Li-Chen Wang, Wei-Li Song, and Daining Fang. “Twistable origami and kirigami: from structure-guided smartness to mechanical energy storage”. In: *ACS applied materials & interfaces* 11.3 (2018), pp. 3450–3458.
- [75] Saad Ahmed et al. “Multi-field responsive origami structures: Preliminary modeling and experiments”. In: *International Design Engineering Technical Conferences and Computers and Information in Engineering Conference*. Vol. 55942. American Society of Mechanical Engineers. 2013, V06BT07A028.
- [76] Zhuang Zhang et al. “Bioinspired rigid-soft hybrid origami actuator with controllable versatile motion and variable stiffness”. In: *IEEE Transactions on Robotics* (2023).